Covariance matrix of nucleon-nucleon potential parameters in few-nucleon studies

Yuriy Volkotrub

Ph.D. thesis written under the supervision of dr. hab Roman Skibiński
at the Jagiellonian University, Faculty of Physics, Astronomy
and Applied Computer Science, Kraków,
Thursday 17$^{\text{th}}$ September, 2020

Contents

Overview of the thesis

One of the main goals of theoretical low-energy nuclear physics is to establish the structure of the nuclear Hamiltonian. Up to now, a large set of experimental data has been accumulated, both from elastic and inelastic nucleons scattering on nuclei over a wide range of energy. This is especially true for the elastic nucleon-deuteron (Nd) scattering and the nucleon-induced deuteron breakup processes. During many years of theoretical investigations of three-nucleon (3N) systems conducted among others, by the Kraków-Bochum group, it was proved that using nucleon-nucleon (NN) force is not sufficient to provide an accurate description of such systems. An additional 3N force (3NF) is required to obtain a precise description of the 3N data [1]. Nowadays, unfortunately, the details of 3N force are still poorly known and many efforts are undertaken to establish their properties. One example are calculations performed in the Kraków-Bochum group that enabled experimentalists to prepare measurements sensitive to specific features of the nuclear Hamiltonians, the role of particular NN force components, charge independence breaking, and the structure of the 3NF. Major important results obtained before the mid-1990s for the 3N system were summarized in a review paper [2], which is an important reference for a reader interested in 3N calculations.

Moreover, in order to obtain reliable and accurate information from comparing 3N data with rigorous theoretical calculations it is necessary to estimate the uncertainties of theoretical predictions, in addition to the uncertainties of 3N data. Such estimation should start already when working with two-nucleon forces only. This would allow to estimate a contribution of 3NF in the description of various phenomena of nuclear physics. Of course such estimations should be confirmed by calculations which explicitly take into account NN interactions combined with 3NFs.

In the past, for various reasons, the uncertainty budget for theory calculations in nuclear physics was not available or the estimated uncertainties did not offer a statistical interpretation. With the increasing accuracy of experimental data in all areas of physics, for example in the three-nucleon sector, see, e.g., Refs. [3, 4, 5, 6, 7], the question of the uncertainty of theoretical predictions has became very relevant in the last decade. For instance, the problem of uncertainty quantification of theoretical calculations was emphasized in an editorial in Physical Review A [8] journal which covers atomic, molecular, and optical physics. This guideline was also taken by the nuclear physicist community. As a result of intensive discussion, among others, the ISNET workshops (Information and Statistics in Nuclear Experiment and Theory) are organized in order to discuss issues related to the application of applied mathematics, information theory and statistics in the analysis of experiments, and possibilities of calculating the uncertainties of relavent theoretical calculations. The first workshop resulted in a special issue of the *Journal of Physics G: Nuclear and Particle Physics* (2015). Additionally, in the near future, the next *J Phys G* special issue devoted to this subject will be published. In my studies I would like to contribute to these efforts and an important part of my thesis is devoted to

studying some specific theoretical uncertainties.

For a specific case of elastic Nd scattering, the *ab initio* theoretical studies of 3N observables are possible using modern models of nuclear forces. NN force models used in such investigations contain a number of free parameters whose values are fixed from the 2N data. For my studies, the most important examples of such models are the new generation of the chiral interaction derived even beyond to the fifth-order (N^4LO) of the chiral expansion using the semilocal regularization in momentum space (SMS) by the Bochum-Bonn group [9] and the semi-phenomenological One-Pion-Exchange-Gaussian (OPE-Gaussian) potential, proposed by the Granada group [10]. This choice is dictated by the availability of the covariance matrix for free parameters of these forces. The knowledge of the covariance matrix of the potential parameters opens new opportunities in studies of few-nucleon systems. One of them, realized in this thesis, is to determine the magnitude of uncertainty of the investigated observables (a so-called theoretical statistical error) that arises from the propagation of uncertainty of NN potential parameters. Part of the results presented in the thesis has been shown in [11, 12]. Another possibility is to investigate correlations among various 2N and 3N observables as well as between observables and specific potential parameters. The information about correlations among such observables is particularly interesting in the context of determining free strength parameters present in the 3N interaction. The values of these parameters are traditionally obtained by fixing from 3N data. However, using correlated 3N observables in such an analysis may lead to an inaccurate determination of the sought parameters. In this thesis I determine the correlations among 3N observables in a statistically correct way, based on the relatively big sample of predictions.

Summarizing, the main goal of this doctoral dissertation is the theoretical study of 3N observables for elastic and inelastic Nd scattering by using the newest semilocal momentum-space regularized chiral force. The first part of this work deals with various types of theoretical uncertainties of the 3N scattering observables. The statistical uncertainties obtained with the OPE-Gaussian potential and the chiral SMS interaction at different orders of chiral expansion are in the heart of my work. In addition to the *nd* elastic scattering, the statistical uncertainties are compared with the truncation errors arising from the restriction to a specific order of chiral predictions, which can be done in two ways using a prescription suggested in [13, 14] or within the Bayesian method [15], and with the cutoff dependence of chiral predictions. The second part of my thesis is devoted to collecting information about the correlations among all 2N and 3N elastic scattering observables as well as between observables and specific potential parameters. The knowledge, if some observables are or are not correlated, can impact future methods of fixing free parameters of the two- and many-body potentials. Especially the case of correlations in a 3N system should deliver information on possible restrictions on data sets used during fitting the 3NF parameters. In the case of correlations between potential parameters and 2N observables, the problem at hand is existence of observables that show strong sensitivity to a given part of the potential. If this is a case such an observable could be possibly used to fix this particular parameter. This, in turn, will reduce the number of remaining free parameters, which would simplify the rest of fitting procedure.

In the next Chapter I give a more elaborate introduction to my studies while in Chapter 2 I describe the two-nucleon force models which are used in investigations. In Chapter 3 I describe various types of theoretical uncertainties and usefulness of covariance matrix of two-nucleon potential parameters. In Chapter 4 I show the essential elements of our methods in computing the deuteron binding energy and 2N scattering observable,

and the framework of the 3N Faddeev equations in computing 3N scattering observables used in my research. Chapter **??** is devoted to results for elastic scattering and breakup reactions. In Chapter **??** I show investigated correlations among various two- and three-nucleon observables as well as between observables and specific potential parameters. I summarize in Chapter.

Chapter 1

Introduction

Modern physics tells that there are four fundamental forces which can describe all observable the Universe. There are gravitational, electromagnetic, strong and weak interactions. Three of them are combined to the Standard Model, except the gravitational one. A scale comparable to a size of no more than the size of atomic nuclei is a field studied within the nuclear physics in close connection with the particle physics.

Nuclear physics studies the properties and structure of atomic nuclei and their reactions. Some of its main tasks are related to the analysis of the nature of nuclear forces acting between nucleons (protons and neutrons) that form nuclei and to identify and explain the properties of their motion. Understanding nuclear forces is fundamental for both theoretical and experimental nuclear physics as well as for applied nuclear physics, in particular for nuclear medicine. Currently, it is known that nuclear interaction between nucleons is a residual interaction of the strong interaction between even finer elements of matter — quarks and gluons and which is described by the Quantum Chromodynamics (QCD). As is well known, nowadays we are not able to solve QCD in the non-perturbative region (at the low-energy scale) and thus to describe processes at nuclear scale starting from quarks and gluons and their interactions. For the first ongoing attempts in lattice QCD, see e.g. Refs. [16, 17]. For example, the obtained deuteron binding energy is still much larger than the experimental value [18, 19]. Another advanced approaches, like the Lattice Effective Field Theory [20], also fail to deliver results of quality comparable with the standard nuclear physics techniques. By the latter ones we understand approaches based on the effective nuclear interactions defined as interactions among nucleons and relying mainly on meson exchange processes.

As a result, effective and phenomenological models of nuclear interactions are still of great importance in low-energy nuclear physics [1] and various *ab initio* techniques to obtain predictions have been derived. Calculations within the *ab initio* or *microscopic* techniques mean that the nuclear A-few body problem can be formulated in terms of the nonrelativistic Schrödinger equation using various NN local or non-local interactions with or without the inclusion of many-body forces. Independently on the problem in hand: the bound state of nucleons, nuclear reactions, production or decay processes, the starting point of research is a construction of the complete Hamiltonian of the system of interacting particles. This thesis is devoted to purely nucleonic processes, in particular, to three-nucleon processes: the elastic and inelastic neutron-deuteron scattering.

[1] In my doctoral research, done as part of the investigations within the Kraków's group, low-energy nuclear physics is understood as nuclear physics at energies below the pion production threshold.

The general form of the nuclear Hamiltonian for the system A of nucleons is

$$H = \sum_{i=1}^{A} \frac{p_i^2}{2m_i} + \sum_{i,j}^{A} V_{ij}^{2\mathrm{N}} + \sum_{i,j}^{A} V_{ijk}^{3\mathrm{N}} + \ldots + V^{A\mathrm{N}} \ , \tag{1.1}$$

where the first term is the non-relativistic kinetic energy, m_i and p_i are the i-th nucleon mass and momentum, respectively, and $V_{ij}^{2\mathrm{N}}$, $V_{ijk}^{3\mathrm{N}}$ and $V^{A\mathrm{N}}$ represent the two-, three and A-nucleon potentials, respectively. The definition (1.1) is used e.g. for a bound state $|\Psi_A\rangle$ in the time-independent Schrödinger equation formulated as an eigenvalue problem $|\Psi_{\mathrm{bound}}\rangle$

$$H\,|\Psi_A\rangle = E\,|\Psi_A\rangle \ , \tag{1.2}$$

where E is the binding energy.

There are a few mathematical algorithms and *ab initio* approaches with well-controlled approximations for solving a A-nucleon Schrödinger equation for light nuclei. In general, this equation can be considered in coordinate or momentum space. Some examples of *ab initio* methods for calculations of few-nucleon systems with $A \geq 4$ were listed and reported in an overview [21]. For example, one of these methods is approach basing on the Faddeev-Yakubovsky equation, which was used to calculate the binding energy and the wave function of ^{4}He [22]. I would like also to mention methods which are quite precise in describing the properties of light and medium mass nuclei up to $A = 12$, i.e. methods based on Monte Carlo algorithms, such as the Monte Carlo variational (VMC) or the Monte Carlo with Green's function (GFMC) methods, see Ref. [23]. It is also worth mentioning that there are methods associated with the shell model of nuclei, as the no-core shell model (NCSM) [24], the No-Core Configuration Interaction (NCCI) [25] model, or the realistic shell model (RSM) [26]. In the last decade, many efforts have been made to use the Similarity Renormalization Group (SRG) approach with a combination of the chiral interaction, see e.g. Ref. [27]. The SRG approach is based on the unitary transformation of the many-body Hamiltonian system to decouple states with high and low momenta [28, 29]. Such transformed Hamiltonian can be next used in the above-mentioned computational schemes. In the case of $A \leq 4$ nuclear bound systems, the hyperspherical harmonic (HH) method has been developed and applied by the Pisa group [30].

The latter method can also be applied to describe the elastic Nd scattering at the very low (≤ 10 MeV) incoming nucleon laboratory energies, working in coordinate or in momentum space [31, 32]. However, to study 3N scattering a few *ab initio* approaches based on the Faddeev equations scheme [33] are currently the most effective tool. The Kraków-Bochum group developed the Faddeev formalism for rigorous calculations applied to 3N continuum observables, see Ref. [2] for a general overview. Interesting computational technique based on the 3N continuum Faddeev calculations with lattice-like discretization in momentum space was developed in [34]. In 3N systems as well as beyond them, the Faddeev formalism can be realized in a couple of ways, like the Alt-Grassberger-Sandhas (AGS) equations [35] with the possibility to include the Coulomb interaction between protons [36] and the Faddeev-Yakubovsky for five-nucleon calculations [37]. Another recent overview of state-of-the-art *ab initio* calculations of the bound state and scattering observables is given in Ref. [38] and references therein.

The deuteron is the only one stable bound state of two nucleons [2]. Analyzing its

[2]It should also be noted that there is a state consisting of two bound protons (di-proton) [39], which

properties, it was found that nuclear forces of short-range nature with a range of not more than $2 \div 3$ fm. The experimental data on the nuclei and nuclear reactions, including a huge amount of data on nucleon-nucleon (proton-proton and proton-neutron) scattering, led to the conclusion that nuclear forces can be considered in the first approximation as a two-particle interaction. Thus, the problem of describing nuclear interactions can be approximately formulated as a problem of determining the two-nucleon (2N) potential V^{2N}.

In general, no matter what strategy (phenomenology, meson exchange picture, etc.) is chosen to build a model of nuclear interactions, the properties of nuclei are taken into account. With increasing number of nucleons, the volume of nuclei increases proportional to the mass number ($A > 4$), what is explained by the fact that the central nuclear force is a short-range force and strongly attractive at this range. This is a saturation effect. The nuclear force depends not only on the range between nucleons (central force), but also on the mutual orientation of spins (spin-spin force), the mutual direction of the spin and the orbital angular momentum (spin-orbital force), and also on the orientation of the spins of each nucleon to the relative distance between them (tensor force). The existence of a spin-orbit force helps to explain the experimentally observed magic numbers for nucleons. Specifically, the presence of a quadrupole moment in the deuteron is result of a tensor force contribution. It is also often convenient to split the nuclear force to a sum of two (short- and long-range) or three (short-, intermediate- and long-range) terms.

The first non-trivial model of nuclear force was the NN potential developed by Hideki Yukawa [40]. Yukawa used the idea that the nucleons interact via exchanges of unknown particle, and combined it with the idea of the short-range interaction. He predicted that this particle should obey the Einstein-Bose statistics and estimated its mass. Today, we identify this particle as the π^0-meson pseudoscalar boson (with total spin 0 and odd parity). Further development of nuclear forces show by the end of the 60s that the NN interaction includes not only a one-pion interaction but also with two pion processes, and much heavier mesons exchanges depending on the inter-nucleon distance. In the 90s, the most known and frequently used the meson-exchange NN models were the Paris potential [41], the Bonn potential [42], and two potentials provided by the Nijmegen group — the non-local Nijmegen potential (Nijm I) and its the local version (Nijm II) [43]. During works on their potential, the Nijmegen group collected 1787 *pp* data and 2514 *np* data and applied a 3σ-rejection criterion and other statistical methods to make the database self-consistent. They performed partial-wave analysis (PWA93) below 350 MeV and the Nijmegen database (or the 1992-database) was obtained. Due to this, they were able to describe 2N scattering data using their potentials with $\chi^2/\text{datum} \approx 1.08$. All above-mentioned models combine a meson exchange theory with a phenomenological approach in the derivation of NN potentials which base upon the operator structure. In general, such a phenomenological NN potential consists of linear combinations of terms which are deduced from the nuclear properties and symmetries. An interested reader can find more detailed information on how the theory of nuclear structure has developed from a historical perspective, from the discovery of the neutron to the present day, as well as a review of NN interactions in Refs. [44, 45, 46, 47, 48].

At the beginning of the 21st century, the most successful *realistic* models of the NN force were the above-mentioned Nijmegen (I, II), the Argonne V18 (AV18) [49] and the CD-Bonn [50] potentials which provided an accurate description of the 2N scattering data

can be considered as the isotope ^{2}He of helium but its lifetime is very short. As for the two bound neutrons (di-neutron), at the moment there is no experimental evidence of its existence.

and deuteron properties. In the case of the AV18 the long-range part of the interaction, given by the one-pion-exchange (OPE), was supplemented by a purely phenomenological short-range part. For the CD-Bonn model the short-range part was described via exchanges of heavier mesons and processes with multiple meson exchanges. The AV18 and the CD-Bonn potentials have 40 and 43 potential force parameters, respectively. The AV18 potential parameters were fitted using the above-mentioned Nijmegen PWA93 results. Before the year 2000, the new sets of experimental 2N data were collected and together with the 1992-database built the 1999-database [50]. The resulting 1999-database was taken into account to construct the CD-Bonn potential. The quality of description can be quantified by the magnitude of χ^2/datum obtained from a comparison of theoretical predictions and experimental data. In the case of the AV18 potential χ^2/PWA92 = 1.09 and χ^2/PWA99 = 1.21. For the CD-Bonn model χ^2/datum = 1.02 for both databases [50]. For the both potentials, only the central values of the parameters were determined and no information about their uncertainties, to the best of our knowledge, was published. In the course of time, the expectations of the improvement in the accuracy of the fitting as well as in establishing parameter uncertainties procedure grew.

The important step in establishing the 2N potential parameters was taken by Rodrigo Navarro Pérez and his collaborators from the Granada group, who carefully revised the whole 2N database. They prepared a new database (Granada-2013 database) [51], removing from the previously used data, those for which the experimental uncertainties had been unknown or unclear defined. They excluded also data sets inconsistent with other data, which led to the self-consistency of the eventually accepted data. The procedure is described in Chapter 2.1 in more detail. The extended statistical tests of this database presented in [51] confirmed the internal consistency of the accepted data. The Granada-2013 database is currently a standard set of data used for fixing parameters of the NN forces what can be done by fitting parameters to the extracted phase shifts or to 2N data directly. The free parameters of the both models of the NN force used in this thesis: the OPE-Gaussian [10] and the family of the chiral SMS interactions from the Bochum group [9] have been fixed with the Granada-2013 database. Specifically the OPE-Gaussian potential has been derived already by R. Navarro Pérez from Granada. This potential is discussed in Chapter 2.1 in detail.

Currently, the most sophisticated models of nuclear forces at the low-energy regime are chiral interactions. S. Weinberg was the first who proved, in his seminal papers [52, 53], that it is possible to build Lagrangian for all possible interactions between pions and nucleons in agreement with the symmetries (including the broken chiral symmetry) and properties of low-energy QCD, and to construct effective Hamiltonian in terms of nucleons and pions. In this construction an infinite number of terms corresponding to the Feynman diagrams for the Lagrangian can be rewritten as an pertubative expansion with respect to some parameter. Each term in this Lagrangian is multiplied by the corresponding coupling constants, the so-called low-energy constants (LECs), which needs to be determined from experimental data in nucleonic or π-N sector [9, 54]. The power counting scheme allows to organize a perturbative ordering of the Lagrangian terms and thus point terms dominant in the potential. The expansion parameter depends on the ratio between the low- and high-energy scales. It is assumed to have the form $Q = \max\left(\frac{p}{\Lambda_\chi}, \frac{m_\pi}{\Lambda_\chi}\right)$, where Λ_χ is the chiral symmetry breaking scale, whose value is a priori set of the order of ρ-meson mass (Λ_χ = 770 MeV), however, values in range 600 MeV [55] – 1 GeV [56] are used [9], [57], [58]. Further $p \equiv |\vec{p}|$ is the magnitude of the external (nucleon) three-momenta in the center of mass scattering system (c.m.s), and

m_π is the pion mass. Important feature of the chiral expansion in powers ν of (Q/Λ_χ) is a finite number of diagrams at a given order which make theory computable. Finally, an effective potential can be derived from the effective Lagrangian with e.g. the method of unitary transformations [59, 54]. This leads to nuclear forces emerging as a hierarchy controlled by the ν, see Figure 1.1, and gives a nice explanation of various stength of contributions to two- and many-body forces obtained within the Chiral Effective Field Theory (χEFT). In general, the expansion of the NN force has the form

$$V_{\rm 2N} = V_{\rm 2N}^{(0)} + V_{\rm 2N}^{(2)} + V_{\rm 2N}^{(3)} + V_{\rm 2N}^{(4)} + V_{\rm 2N}^{(5)} + \dots \ , \tag{1.3}$$

with the superscripts referring to the power ν of the expansion parameter $(Q/\Lambda_\chi)^\nu$. For example, in the lowest leading order ($\nu = 0$) the NN potential is made up by two terms, represented by the graphs in the first row of Figure 1.1. They are the static one-pion exchange ($V_{1\pi}$) and the contact interaction ($V_{\rm cont}$) between two nucleons. The latter plays the role of a short-range interaction. For $\nu = 1$ all terms cancel and give no contribution to the NN interaction. At the higher orders of the chiral expansion more terms containing multiple mesons exchanges and various types of contact terms occur. At the next-to-next-to-leading order (N^{2}LO), which corresponds to $\nu = 3$, the NN potential involves contributions from the one-, two-exchange and contact terms with up to three derivatives which enters new short-range interactions contributing at this order. In addition, for a 3N system a 3N force appears, for the first time, at this chiral order.

Nowadays, there are few groups engaged in derivation of chiral forces and two of them have dominated the field: the Bochum-Bonn group (see Refs. [55, 60, 61, 62] and more recently [9]) and the Moscow(Idaho)-Salamanca group (see Refs. [56, 63, 64, 65, 66]). Both teams start from the same Lagrangian but due to various methods used, their final potentials differ.

The important difference between their approaches is using various ways of regularization of the chiral nuclear potential. In particular, the Moscow(Idaho)-Salamanca collaboration uses a non-local regularization procedure in momentum-space for both the long- and short-range contributions [56]. The regulator function of the initial p and final p' relative momentum of two nucleons is taken as

$$f(p', p) = \exp\left[-\left(\frac{p'}{\Lambda}\right)^{2n} - \left(\frac{p}{\Lambda}\right)^{2n} \right] \ , \tag{1.4}$$

where n depends on the chiral operators (e.g., $n = 4$ for the one-pion exchange potential). The three values of the cutoff parameter $\Lambda = 450$, 500, and 550 MeV were used while fitting potential parameters which resulted in three versions of this potential [56]. Obtained χ^2/datum values depend on the regularization parameter Λ, the order of chiral expansion, the energy range, and the isospin channel. In the case of the next-to-next-to-next-to-next-to-leading order (N^{4}LO) potential and $\Lambda = 500$ MeV, χ^2/datum = 1.15 for the fit of the 2016-database [3] (see [56] for details) of combined np and pp data in the energy range 0–290 MeV.

In their first works, the Bochum-Bonn group also proposed and used a non-local regulator. However, due to observed strong artefacts the newest models of the Bochum-

[3] 2016 database bases on the 1999 database and consists of 2932 pp and 3058 np data and including the data published between 2000 and 2016 which are not discarded by the Nijmegen criteria [67].

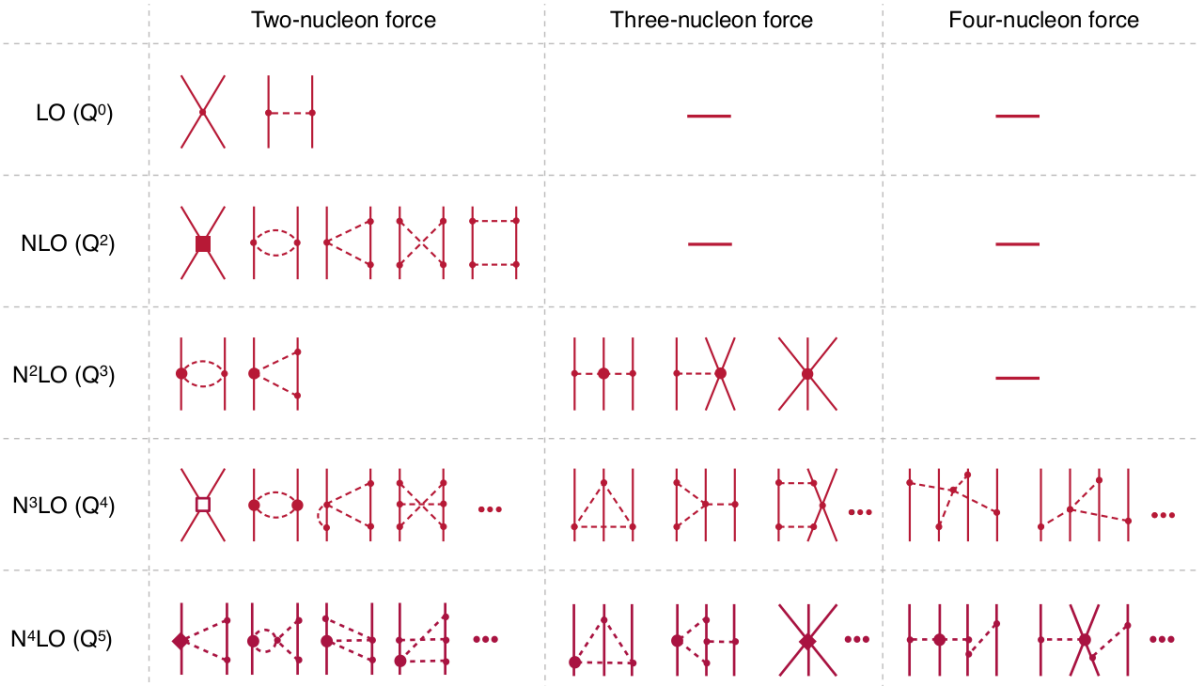

Figure 1.1: Hierarchy of nuclear forces in χEET at increasing orders in chiral expansion based on the Weinberg scheme. Figure is taken from Ref. [54]. Solid and dashed lines represent nucleons and pions, respectively. Solid dots, filled circles, filled squares, filled diamonds, and open squares denote vertexes arising at corresponding order ν_i $(i = 0, 2, 3, 4, 5)$ of the effective Lagrangian, respectively. (Image source: `https://www.frontiersin.org/files/Articles/515888/fphy-08-00098-HTML/image_m/fphy-08-00098-g002.jpg`; use permitted under the Creative Commons Attribution License CC BY 4.0.)

Bonn group, use the semilocal [4] regularization. It can be applied either in coordinate space with the regulator function,

$$f(r) = \left[1 - exp\left(-\frac{r^2}{R^2}\right)\right]^6 , \tag{1.5}$$

where r is the internucleon distance and R is the regulator parameter, [55, 62]; or in momentum space by changing the meson propagator, see Ref. [9].

In this thesis I use the chiral NN potentials up to N^4LO^+ order (the N^4LO potential supplemented by some terms from the sixth order N^5LO force) with regularization applied in momentum space (the SMS forces). This force is described in Chapter 2.2 in detail.

The understanding of nuclear systems is limited if using only NN potentials beyond 2N systems. In principle, the NN potentials can well describe 3N systems, and most of the results are in good agreement with the available experimental data at laboratory nucleon scattering energies of up to 100 MeV [2]. However, there are some large discrepancies between theory and experiment already in the 3N system, for example, the triton binding energy problem [68, 69, 70], the A_y-puzzle (the problem of describing the nucleon

[4]The term “semilocal" means which the nuclear force is regularized locally for the long-range part and non-locally for the short-range one.

analyzing power for the elastic Nd scattering up to 30 MeV) [71], and the description of the deuteron breakup cross section for the symmetric space star (SST) and quasi-free scattering (QFS) configurations [72, 73]. Therefore, in order to obtain a more accurate description of 3N system, a NN interaction must be supplemented by a 3N force acting in this system.

Among all of the many-nucleon forces, the 3N force is the most intensively studied, but its structure is still unclear. Currently, the important models of 3NF are the semi-phenomenological ones: the Tucson-Melbourne [74, 75, 76] force, the UrbanaIX [77] potential and models arising from χEFT. The latter have been derived mainly by the Bochum-Bonn group, starting from the seminal paper [78] where the 3NF effects in the nucleon-deuteron scattering up to the next-to-next-the leading order (N^2LO) were investigated. The 3N interaction, similarly to the two-nucleon one is derived within the chiral approach in a perturbative way [61, 63]. It occurs for the first time at the N^2LO and has at this order only two free parameters, (the low-energy constants commonly denoted c_D and c_E). Already in the work [78] the problem of fixing of these parameters had to be addressed. The authors chose the ^{3}H binding energy and the nucleon-deuteron doublet scattering length $^2a_{nd}$ to find c_D and c_E values. The same procedure to fix c_D and c_E was also used at the next (N^3LO) order of chiral expansion with new diagrams for 3NF taken into account [79]. These new contributions to the 3NF do not introduce new free parameters, however at the next (N^4LO) order again several free parameters are expected [80]. Another strategy of fixing 3NF's parameters was used recently for the next generation of the chiral models — with semilocal regularization in coordinate space [27]. At the moment the 3NF with regularization in coordinate space is available only up to N^2LO and this dominant 3NF contribution is used in [27]. Here, beside the ^{3}H binding energy, the total and differential cross sections at $E = 70$ MeV and at $E = 108$ MeV around its minimum were used to fix the c_D and c_E parameters. The use of the cross section instead of the nucleon-deuteron doublet scattering length was imposed by the strong correlation between the ^{3}H binding energy and the nucleon-deuteron doublet scattering length (the so-called Phillips line) [81], which could bias the fitting procedure and lead to incorrect c_D and c_E values. The choice of the cross section as the new observable was dictated by the fact that big 3NF effects are observed for this observable above $E \approx 60$ MeV, thus a sensitivity of theoretical predictions to the values of free parameters had been expected. Another reason for using the cross section was the existence of the very precise experimental data [82]. Nevertheless, the values of c_D and c_E obtained in [27] suffer from relatively large uncertainties and are (for the regulator parameter $R = 0.9$ fm): $c_D = 2.1 \pm 0.9$ and $c_E =$ -0.329 (+0.103, -0.106), so the uncertainty amounts up to 30%-40%, being quite substantial. The magnitudes of the free parameters and their uncertainties depend also on the value of the regulator parameter and for $R = 1$ fm one finds $c_D = 7.2 \pm 0.9$ and $c_E =$ -0.381 (+0.117, -0.122), so the uncertainty here reaches 12%-30%. Such big values of parameters' uncertainties suggest that usefulness of other observables to fix 3NF free parameters is worth investigating as it can lead to a more precise determination of the c_D and c_E values.

Investigation of Nd scattering within the Faddeev equations in momentum space is a good tool to study not only NN potential but also 3N force. A comprehensive overview of 3N calculations with various semi-phenomenological NN potentials is given in Ref. [1]. Similar works were recently conducted as part of the LENPIC (Low-Energy Nuclear Physics International Collaboration project) by applying the chiral interaction [13, 14, 27] with the coordinate space semilocal regularization (the SCS potential) [55] and with the

momentum space semilocal regularization (the SMS potential) [9, 58].

During the last ten years, in parallel to the development of the nuclear force models, the question how to estimate the uncertainties of predictions is also being considered. For example, various ideas for estimating theoretical uncertainties have been proposed and discussed within the χEFT framework, see Refs. [15, 55, 57, 83, 84]. In Ref. [61] a simple approach for estimating the theoretical uncertainty in few-nucleon calculations by the cutoff dependence was suggested. However, as was shown by E. Epelbaum, H. Krebs, and Ulf-G. Meißner (EKM) [55], such procedure has some disadvantages, namely does not allow one to evaluate precisely the effects of neglected interactions. Therefore in [55], they proposed and applied for 2N observables new method ("EKM prescription") for estimating truncation errors, which are uncertainties arising from neglecting higher orders of the chiral expansion for the 2N potential. This algorithm was adopted also for many-nucleons systems, in the cases where predictions are based on a NN interaction [13, 14] only orr on NN+3N force [27]. However, since the EKM prescription does not provide a statistical interpretation of truncation errors, a Bayesian approach for calculating the posterior probability distribution for predictions in the chiral EFT was developed, see Refs. [15, 57] focused only on 2N observables.

As mentioned above, there is one more additional source of theoretical errors — the statistical errors arising from the propagation of uncertainties of free parameters of a NN interaction. For the first time, it was studied with the OPE-Gaussian potential in the description of the elastic Nd observables [11]. In recent paper [12] we investigated the magnitudes of statistical uncertainties of 3N observables of the elastic and inelastic Nd scattering at energies up to 200 MeV predicted by the chiral SMS potential at different orders of chiral expansion up to N^4LO^+. Last but not least, there are the uncertainties arising from using the various models of nuclear interaction and the numerical uncertainties as well as the uncertainties bound to the computational scheme used. As was shown in Ref. [11] the two latter are small in the Faddeev approach we use. Study of the dependence of 3NF predictions on various potentials is out of scope of this thesis where we restrict only to the chiral SMS NN and the OPE-Gaussian interactions. The choice of these models is dictated by the fact that the authors quantified the statistical uncertainties of NN potential parameters and obtained not only their values but also their covariance matrices. For these forces I will discuss the dependence of prediction on used interactions as well.

Chapter 2

NN potentials

2.1 The OPE-Gaussian potential

The OPE-Gaussian force is a phenomenological NN potential which has been presented by R. Navarro Pérez, J. E. Amaro, and E. Ruiz Arriola in 2014 [10]. In usuall way, this potential can be decomposed to the short-range $V_{\rm short}(r)$ and the long-range $V_{\rm long}(r)$ parts,

$$V(r) = V_{\rm short}(r)\theta(r_c - r) + V_{\rm long}(r)\theta(r - r_c) \ , \tag{2.1}$$

where r is the internucleon distance and for the OPE-Gaussian potential $r_c = 3$ fm.

The long-range force $V_{\rm long}(r)$ is, in turn, the sum of the one-pion exchange (OPE) force and the electromagnetic (EM) corrections:

$$V_{\rm long}(r) = V_{1\pi} + V_{\rm EM} \ . \tag{2.2}$$

The OPE potential $V_{1\pi}$ is the same as the charge-dependent OPE potential used in the PWA93 by the Nijmegen group [85] and the AV18 potential [49] which reads as

$$V_{1\pi}(r) \equiv V_{m,1\pi}(r) = \frac{1}{3} m f^2 \left(\frac{m}{m_s}\right)^2 \left[Y_m(r)\vec{\sigma}_1 \cdot \vec{\sigma}_2 + T_m S_{1,2}\right] \ , \tag{2.3}$$

where $\vec{\sigma}_1$ and $\vec{\sigma}_2$ denote the Pauli matrices of nucleons 1 and 2, respectively, $S_{1,2}$ is the tensor operator, and $Y_m(r)$ and $T_m(r)$ are the Yukawa and tensor functions,

$$\begin{aligned} S_{12} &= 3\left(\vec{\sigma}_1 \cdot \hat{r}\ \vec{\sigma}_2 \cdot \hat{r}\right) - \vec{\sigma}_1 \cdot \vec{\sigma}_2 \ , \ \hat{r} = \frac{\vec{r}_1 - \vec{r}_2}{|\vec{r}_1 - \vec{r}_2|} \ , \\ Y_m(r) &= \frac{e^{-mr}}{mr} \ , \\ T_m(r) &= \frac{e^{-mr}}{mr}\left(1 + \frac{3}{mr} + \frac{3}{(mr)^2}\right) \ . \end{aligned} \tag{2.4}$$

The scalling mass m_s in Eq. (2.3) is the charged-pion mass $m_{\pi^\pm}$, the average value of the pion mass $m = \frac{1}{3}(m_{\pi^0} + 2m_{\pi^\pm}) = 138.057$ MeV, $f = \sqrt{0.075} \approx 0.274$ is the pion coupling constant, for all pairs of nucleons (pp, np, nn). As a result, charge dependence is yield only due to the difference between the charged $m_{\pi^\pm}$ and neutral m_{π^0} pion mass and leads

to

$$V_{1\pi}^{pp}(r) = V_{1\pi}^{nn} \neq V_{1\pi}^{np} \ . \tag{2.5}$$

The EM corrections correspond to the np and pp potentials. The np potential contains only a magnetic moment (MM) interaction

$$V_{\rm EM}^{np} = V_{\rm MM}^{np}(r) = -\frac{\alpha\mu_n}{2m_n r^3}\left(\frac{\mu_p S_{1,2}}{2m_p} + \frac{\vec{L}\cdot\vec{S}}{\mu}\right) \ , \tag{2.6}$$

where m_n and m_p are the neutron and proton masses, μ is the reduced mass of the nucleon, μ_n and μ_p are the neutron and proton magnetic moments, $\vec{L}$ and $\vec{S}$ denote the angular momentum and spin operator, respectively, and $\vec{L}\cdot\vec{S}$ is the 2N spin-orbit operator. The pp EM potential contains one- and two-photon exchange, vacuum polarization and a magnetic moment interaction

$$V_{\rm EM}^{pp} = V_{\rm C_1}^{pp}(r) + V_{\rm C_2}^{pp}(r) + V_{\rm VP}^{pp}(r) + V_{\rm MM}^{pp}(r) \ , \tag{2.7}$$

with detalied expressions given in Eqs. (9-12) of Ref. [51]

Below $r_c = 3$ fm the short-range part $V_{short}(r)$ of the OPE-Gaussian force is built from 18 spin-isospin operators $\hat{O}_n$, 16 of these operators are the same as in the AV18 model [43]. Among them 14 operators are charge-independent,

$$\begin{aligned}\hat{O}_{i\in[1,14]} =&\{\mathbb{1}, \vec{\tau}_1\cdot\vec{\tau}_2, \vec{\sigma}_1\cdot\vec{\sigma}_2, (\vec{\sigma}_1\cdot\vec{\sigma}_2)(\vec{\tau}_1\cdot\vec{\tau}_2), S_{12}, S_{12}(\vec{\tau}_1\cdot\vec{\tau}_2),\\ &\vec{L}\cdot\vec{S}, \vec{L}\cdot\vec{S}(\vec{\tau}_1\cdot\vec{\tau}_2), \vec{L}^2, \vec{L}^2(\vec{\tau}_1\cdot\vec{\tau}_2),\\ &\vec{L}^2(\vec{\sigma}_1\cdot\vec{\sigma}_2), \vec{L}^2(\vec{\sigma}_1\cdot\vec{\sigma}_2)(\vec{\tau}_1\cdot\vec{\tau}_2), (\vec{L}\cdot\vec{S})^2, (\vec{L}\cdot\vec{S})^2(\vec{\tau}_1\cdot\vec{\tau}_2)\} \ .\end{aligned} \tag{2.8}$$

The remaining operators

$$\hat{O}_{i\in[15,18]} =\{T_{12}, (\vec{\sigma}_1\cdot\vec{\sigma}_2), \vec{L}^2 T_{12}, \vec{L}^2(\vec{\sigma}_1\cdot\vec{\sigma}_2)T_{12}\} \ , \tag{2.9}$$

with $T_{12} = 3\tau_{z1}\tau_{z2} - \vec{\tau}_1\cdot\vec{\tau}_2$ introduce charge dependence. Each element of sets (2.8-2.9) is multiplied by a sum of four Gaussian functions $F_{i,n}(r) = V_{i,n} exp(-r^2/(2a_i^2))$, where $a_i = \frac{a}{1+i}$ and $V_{i,n}$ are the strength coefficients. Thus

$$V_{\rm short}(r) = \sum_{n=1}^{18} \hat{O}_n \left[\sum_{i=1}^{4} V_{i,n} F_{i,n}(r)\right] \ . \tag{2.10}$$

It should be noted that in Ref. [10] there are 21 operators, but three of them (tT, τ_z and $\sigma\tau_z$) are almost equal zero in practical calculations [10], [86] and have been skipped in the final version of the OPE-Gaussian potential. The free parameter a, which determines the width of the functions $F_{i,n}(r)$, together with the operator coefficients $V_{i,n}$ were fixed from the data NN collected in Granada-2013 database [51].

The construction of this database was done in the following steps:

1. The Granada group collected 8124 available np- and pp-scattering data taken between 1950 and 2013 in the laboratory energy range $E_{\rm lab}$ up to 350 MeV. They removed data with unknown or unclear statistical and systematic uncertainties.

Operator	$V_{1,n}$	$V_{2,n}$	$V_{3,n}$	$V_{4,n}$
$\mathbb{1}$	-19.28330126	126.28715008	-648.61345585	694.49367435
$\vec{\tau}_1 \cdot \vec{\tau}_2$	2.36233395	-25.47505195	130.03224633	-284.71844492
$\vec{\sigma}_1 \cdot \vec{\sigma}_2$	6.05581487	-75.18832503	372.41961972	-530.80008401
$\tau\sigma$	7.36008330	-48.55160272	273.71591816	-349.00547346
$(\vec{\sigma}_1 \cdot \vec{\sigma}_2)(\vec{\tau}_1 \cdot \vec{\tau}_2)$	1.99828652	-22.12164190	70.84584496	-50.72248959
$S_{12}, S_{12}(\vec{\tau}_1 \cdot \vec{\tau}_2)$	15.02271531	-38.34776035	183.80564790	-160.48060286
$\vec{L} \cdot \vec{S}$	-2.61725312	39.43014573	-217.03270342	-109.64162556
$\vec{L} \cdot \vec{S}(\vec{\tau}_1 \cdot \vec{\tau}_2)$	0.01009424	2.59116238	-26.57555840	-77.56809604
$\vec{L}^2$,$\vec{L}^2(\vec{\tau}_1 \cdot \vec{\tau}_2)$	1.43519736	-23.58906341	67.86552330	144.11773134
$\vec{L}^2(\vec{\sigma}_1 \cdot \vec{\sigma}_2)$	-0.41138176	8.33346137	-82.98819447	175.09618737
$\vec{L}^2(\vec{\sigma}_1 \cdot \vec{\sigma}_2)(\vec{\tau}_1 \cdot \vec{\tau}_2)$	-0.09972181	2.25339230	-51.87819771	175.08890636
$(\vec{L} \cdot \vec{S})^2$	-0.26615545	6.63257735	-55.34306118	100.71528331
$(\vec{L} \cdot \vec{S})^2(\vec{\tau}_1 \cdot \vec{\tau}_2)$	0.46072934	-11.65544792	150.58275714	-302.07573779
$ls2\tau$	0.71538487	-18.88652666	141.73160452	-182.73368764
T_{12}	0.63788724	-7.90421846	24.23180376	-19.73899169
$(\vec{\sigma}_1 \cdot \vec{\sigma}_2)$	-0.63788724	7.90421846	-24.23180376	19.73899169
$\vec{L}^2 T_{12}$	-0.10631454	1.31736974	-4.03863396	3.28983195
$\vec{L}^2(\vec{\sigma}_1 \cdot \vec{\sigma}_2)T_{12}$	0.10631454	-1.31736974	4.03863396	-3.28983195

Table 2.1: The central values of operator coefficients $V_{i,n}$ (in MeV) of the OPE-Gaussian potential. The parameter a is 2.30347728 [fm].

2. They performed the least-squares fitting procedure to this database and the deuteron binding energy by the coarse-grained potential and delta-shell representation for the short and intermediate part of the NN interaction in terms of partial-wave decomposition at given scattering energy and angle [51, 87].

3. Some sets of data were incompatible with each other. To remove them, R. Navarro Pérez and collaborators applied the 3σ-criterion introduced by the Nijmegen group in the PWA93. Namely, for the Gaussian statistical data uncertainties ΔO_i^{data}, the residuals for observables O_i, $\left(O_i^{data} - O_i^{theory}\right)/\Delta O_i^{data}$ should be normal-distributed within a 3σ-confidence level. Unfortunately, this criterion has disadvantages. One of them is that when non-normal outliers data is rejected, it leads to a significantly improved fitting of compatible data (overestimation) [51]. Therefore, they applied the improved 3σ-criterion [51] to the complete database based on the idea of 3σ self-consistent rejection given by Gross and Stadler [88] and again refitted of the parameters. As a result, they obtained the new database (the 3σ self-consistent Granada-2013 database), that incorporates 6713 *pp* and *np* data and confirmed good statistical properties of their χ^2 fit with the value of χ^2/datum = 1.05. Having the database and emerging phase-shifts it was possible to fix 42 free partial-wave parameters of the OPE-Gaussian potential which are linear functions of operator coefficients $V_{i,n}$ [10]. Final, used also in this thesis, values of $V_{i,n}$ are presented in Table 2.1. The resulting χ^2/datum for the OPE-Gaussian force amounts 1.06 as fitted to data listed in Ref. [51]. The performed extensive statistical analysis of data and careful fitting procedures allowed authors of Ref. [89] to provide not only

the values of free parameters but also their covariance matrix [89].

The knowledge of the covariance matrix of parameters allowed authors of Ref. [89] to sample, from the multivariate normal distribution another sets of potentials parameters. They provided us with a sample of 50 sets of parameters $\{V_{i,n}, a\}$ and its central values. Finally, we would like to note, that the OPE-Gaussian potential has a similar structure to the AV18 force and thus it can be regarded as a remastered version of the standard AV18 model.

2.2 The chiral SMS potential

Choosing nucleons and pions as only particles in the theory the chiral NN potential can be written as

$$V_{2N} = V_{\rm cont} + V_{\pi} \tag{2.11}$$

where $V_{\rm cont}$ is the contact interaction between nucleons and V_{π} represents the pion contributions to the two-nucleon potential. The long-range part of nuclear forces is completely determined by the chiral symmetry of QCD and experimental information on pion-nucleon (πN) scattering. Moreover, the pion exchange contributions can be separated by the number of exchanged pions at each chiral order of the chiral expansion, i.e.

$$\begin{aligned} V_{1\pi} &= V_{1\pi}^{(0)} + V_{1\pi}^{(2)} + V_{1\pi}^{(3)} + V_{1\pi}^{(4)} + V_{1\pi}^{(5)} + \dots \ , \\ V_{2\pi} &= V_{1\pi}^{(2)} + V_{1\pi}^{(3)} + V_{1\pi}^{(4)} + V_{1\pi}^{(5)} + \dots \ . \end{aligned} \tag{2.12}$$

As an example I show the OPE potential at order Q^0 (LO) given directly in momentum space reads

$$V_{1\pi}^{(0)}(\vec{q}) = -\left(\frac{g_A}{2F_\pi}\right) \vec{\tau}_1 \cdot \vec{\tau}_2 \frac{\vec{\sigma}_1 \cdot \vec{q}\ \vec{\sigma}_2 \cdot \vec{q}}{q^2 + m_\pi^2} \ . \tag{2.13}$$

Here $\vec{q}$ is the relative momentum transfer of the exchanged pion $\vec{q} = \vec{p}\,' - \vec{p}$, $\vec{p}$ and $\vec{p}\,'$ are the initial and final relative momenta of the two nucleons in the c.m.s, $\vec{\tau}_1$, $\vec{\tau}_2$ denote isospin matrices of nucleons 1 and 2, respectively. $g_A = 1.29$ is the pion-nucleon axial coupling constant and $F_\pi = 92.4$ MeV is the pion decay constant.

Similarly, the contact interaction between nucleons, which plays a role of the short-range part of the NN force takes the form

$$V_{\rm cont} = V_{\rm cont}^{(0)} + V_{\rm cont}^{(2)} + V_{\rm cont}^{(4)} \dots \ . \tag{2.14}$$

The chiral potential with semilocal regularization in momentum space (the SMS potential) has been derived completely up to the fifth-order (N^{4}LO) of the chiral expansion by the Bochum-Bonn group [9]. Comparing the previous chiral forces, the authors fixed the πN low-energy constants (LECs) using the Roy-Steiner analysis [90], skipped redundant contact terms in the higher order of the chiral expansion (starting at order Q^4, i.e. N^{3}LO), and, using the Granada-2013 database, determined adjustable parameters of the potential from *np* and *pp* scattering data and the deuteron binding energy. They also added the four leading contact terms acting in the N^{5}LO (Q^6 order) F-waves from Ref. [56] to their N^{4}LO, potential obtaining so-called N^{4}LO$^+$ interaction.

A general structure of the contact interactions of the chiral SMS force up to fourth-

order (N^3LO) Q^4 is

$$
\begin{aligned}
V_{\rm cont}^{(0)} &= C_S + C_T \vec{\sigma}_1 \cdot \vec{\sigma}_2 \ , \\
V_{\rm cont}^{(2)} &= C_1 q^2 + C_2 k^2 + \left(C_3 q^2 + C_4 k^2\right) \left(\vec{\sigma}_1 \cdot \vec{\sigma}_2\right) + \frac{i}{2} C_5 \left(\vec{\sigma}_1 \cdot \vec{\sigma}_2\right) \cdot \left(\vec{k} \times \vec{q}\right) \\
&\quad + C_6 \left(\vec{q} \cdot \vec{\sigma}_1\right) \left(\vec{q} \cdot \vec{\sigma}_2\right) + C_7 \left(\vec{k} \cdot \vec{\sigma}_1\right) \left(\vec{k} \cdot \vec{\sigma}_2\right) \ , \\
V_{\rm cont}^{(4)} &= D_1 q^4 + D_2 k^4 + D^3 q^2 k^2 + D_4 \left(\vec{q} \times \vec{k}\right)^2 \\
&\quad + \left(D_5 q^4 + D_6 k^4 + D_7 q^2 k^2 + D_8 \left(\vec{q} \times \vec{k}\right)^2\right) \left(\vec{\sigma}_1 \cdot \vec{\sigma}_2\right) \\
&\quad + \frac{i}{2} \left(D_9 q^2 + D_{10} k^2\right) \left(\vec{\sigma}_1 + \vec{\sigma}_2\right) \cdot \left(\vec{k} \times \vec{q}\right) \\
&\quad + \left(D_{11} q^2 + D_{12} k^2\right) \left(\vec{\sigma}_1 \cdot \vec{q}\right) \left(\vec{\sigma}_2 \cdot \vec{q}\right) \\
&\quad + \left(D_{13} q^2 + D_{14} k^2\right) \left(\vec{\sigma}_1 \cdot \vec{q}\right) \left(\vec{\sigma}_2 \cdot \vec{q}\right) \\
&\quad + D_{15} \vec{\sigma}_1 \cdot \left(\vec{q} \times \vec{k}\right) \vec{\sigma}_2 \cdot \left(\vec{q} \times \vec{k}\right) \ ,
\end{aligned}
\tag{2.15}
$$

where $\vec{k} = (\vec{p} + \vec{p}\,')/2$ and C_S, C_T $C_{1,\ldots,7}$ and $D_{1,\ldots,15}$ are the LECs which determine the strength of short-range interaction and should be find from data.

The usage of nuclear forces derived from χEFT in few- and many-body problems demand a local regularization for the pion exchange contributions to reduce the amount of finite-cutoff terms and to avoid divergences after substituting, e.g., into the Lippmann-Schwinger equation. In Ref. [55], the Bochum-Bonn group implemented the regularization of the long-range potential in coordinate space, see Eq. 1.5. Although such regulator allowed to significantly reduce the long-range cutoff terms, but its application turned out to be difficult for the regularization of 3NFs and currents at higher orders of chiral expansion. Therefore, the Bochum group introduced a local regularization scheme of long-range forces in momentum space by emplyoing a regularization of static one-pion exchange contribution [9] in the following way

$$
f(p', p) \propto \exp\left(-\frac{\left(m_\pi^2 - \vec{q}^{\,2}\right)^2}{\Lambda^2}\right) \ , \tag{2.16}
$$

with the cutoff values of $\Lambda = 400, 450, 550$, and 550 MeV. Such approach, as the authors of Ref. [9] argue contributes only to the short-range terms and does not influence the long-range pion exchange potentials.

Implementing local regularization to the long-range potential and multiplying the contact terms with a non-local Gaussian regulator $\exp\left(-\frac{p'^2+p^2}{\Lambda^2}\right)$ in combination with the very detailed fitting procedure of the NN contact LECs leads to a high-quality potential. Specifically, for the chiral SMS potentials of Ref. [9] obtained with the Granada-2013 database [10] the covariance matrices of its free parameters (LECs) at all chiral orders LO-N^4LO^+ have been obtained. The number of free parameters (LECs) is 2, 9, 9, 22, 23, 27 at LO, NLO, N^2LO, N^3LO, N^4LO and N^4LO^+, respectively. Sample visualization of correlations among the various LECs is given in Figure 10 of Ref. [9] for the chiral N^4LO^+ SMS potential with $\Lambda = 450$ MeV.

Currently, the chiral SMS NN potential is the interaction delivering the best description of NN data. For example, the SMS N^4LO^+ with regularization parameter $\Lambda =$

450 MeV gives χ^2/datum = 1.06 (np scattering data) and χ^2/datum = 1.00 (pp scattering data), see Table 4 of Ref. [9] up to 300 MeV. In addition, the availability of covariance matrices of LECs for all chiral cutoffs and orders allows us to study, for the first time for a chiral force, the propagation of uncertainties of NN interaction parameters to 3N continuum observables, see Chapter 3 and Chapter **??**.

Chapter 3

Application of a covariance matrix

In Chapter 1, I have outlined the advantages of using the covariance matrix of NN potential parameters and briefly mentioned types of errors to the Nd scattering observables. In this chapter I discuss the various sources of theoretical uncertainties in the *ab initio* type calculations based on the chiral SMS model at various orders, neglecting the 3N force present in describing the 3N processes. The main results of such study were previously shown in our Refs. [11, 12]. Studies of correlations among all calculated 2N and 3N observables, as well as between observable and specific potential parameters, will also be discussed.

3.1 Uncertainty quantification presented in 3N studies

3.1.1 Determination of statistical uncertainty in a 3N system

As defined in Chapter 1, the statistical uncertainty refers to an error arising from uncertainties of parameters of a given NN interaction. In our method of estimation, computation of the statistical uncertainties requires a big sample of predictions obtained with different sets of parameters within one model of interaction.

The algorithm for determining statistical uncertainty and using it further for the chiral SMS force can be divided into the following steps:

1. Preparation of sets of the potential parameters.

   Having at our disposal covariance matrix for the potential parameters, as well as central values of parameters, I sample 50 sets of the potential parameters from the multivariate normal distribution. The multivariate sampling was done using the Mathematica® [91] computing system (see Appendix **??**). Such a number of sets guarantee a statistically meaningful probe, as will be shown in Chapter **??**.

2. Computing observables for each set of potential parameters

   For each set S_i $(i = 0, 1, \ldots, 50)$ I computed the deuteron wave-function by solving the Schrödinger equation and the t-matrix elements from the Lippman-Schwinger equation and solved the Faddeev equation to construct the transition amplitude from which the 3N observables can be obtained for all investigated models of NN interaction. From solutions of the Lippmann-Schwinger equation 2N observables can be also computed. More details about these calculations will be given in Chapter 4. As a result, the angular dependence of various 3N scattering observables is known for each set of parameters S_i. The obtained predictions can be used to study

(a) for a given observable X at an energy E and at a scattering angle θ, the empirical probability density function of the observable $X(E,\theta)$ resulting when various sets S_i, $(i = 1, \ldots, 50)$ are used;

(b) for a given observable X, both the angular and energy dependencies of results based on various sets S_i.

This, in turn, allows one to find the magnitude of statistical uncertainty of a given 3N observable X and to analyze correlations among all observables.

3. Quantification of the statistical uncertainty

Various estimators can be used to quantify the statistical uncertainty of the observable $X(E,\theta)$. For example, by assuming there are 50 sets of potential parameters:

(a) The sample standard deviation $\sigma(X) = \sqrt{\frac{1}{50-1}\sum_{i=1}^{50}\left(X_i(E,\theta) - \bar{X}(E,\theta)\right)^2}$, where $\bar{X}(E,\theta)$ is the mean value of predictions.

(b) $\frac{1}{2}\Delta_{100\%} \equiv \frac{1}{2}\left(\max\{X_i(E,\theta)\} - \min\{X_i(E,\theta)\}\right)$, where the minimum and maximum are taken over all predictions $\{X_i(E,\theta)\}$ based on 50 sets of LECs $S_i, i = 1, 2, \ldots, 50$.

(c) $\frac{1}{2}\Delta_{68\%} \equiv \frac{1}{2}\left(\max\{X_i(E,\theta)\} - \min\{X_i(E,\theta)\}\right)$, where the minimum and maximum are taken over 34 (68% of 50) predictions based on different sets of LECs. The set of 34 observables is constructed by discarding the 8 lowest and the 8 highest predictions for a given observable and at specific scattering angle and energy.

(d) $\frac{1}{2}$IQR: half of the standard estimator of the interquartile range being the difference between the third and the first quartile IQR $= Q_3 - Q_1$. For the sample of size 50, this corresponds to taking half of the difference between the predictions on 37th and 13th positions in a sample sorted in ascending order.

The estimators $\frac{1}{2}\Delta_{100\%}$ and $\sigma(X)$ are sensitive to possible outliers in the sample, and thus accepting them as estimators of dispersion can lead to overestimation of the statistical uncertainty. On the other hand, due to the fact that the IQR is calculated using only half of the elements in the sample can leads to an underestimation of the theoretical uncertainty. Therefore, we chose $\frac{1}{2}\Delta_{68\%}$ as an optimal measure for dispersion of predictions and consequently as an estimator of the statistical uncertainty [11].

3.1.2 Determination of truncation errors within EKM method

In addition to the statistical uncertainties, also the truncation errors, which play the role of systematic uncertainty can be evaluated. As was outlined in Chapter 1, the truncation errors are uncertainties that arising from restriction to a given order of the chiral expansion. The one way to evaluate truncation errors is using the EKM approach [55]. Consider any 3N scattering observable X which can be expanded up to the k-th order of the chiral expansion Q^k $(k = 0, 2, 3, \ldots)$ but at a fixed cutoff value Λ in the form

$$X = X^{(0)} + \Delta X^{(0)} + \Delta X^{(2)} + \Delta X^{(3)} + \ldots + \Delta X^{(k)} \,, \tag{3.1}$$

where $\Delta X^{(2)} := X^{(2)} - X^{(0)}$, $\Delta X^{(k)} := X^{(k)} - X^{(k-1)}$ with $k > 2$, and $X^{(k)}$ is a prediction obtained at order Q^k.

The truncation error $\delta(X)^{(k)}$ of an observable X at k-th order of the chiral expansion with $k = 0, 2, \ldots$ can be estimated as

$$\begin{aligned}
\delta(X)^{(0)} &\geq \max\left(Q^2|X^{(0)}|\right) \ , \\
\delta(X)^{(2)} &\geq \max\left(Q^3|X^{(0)}|, Q|X^{(2)} - X^{(0)}|\right) \ , \\
\delta(X)^{(k)} &\geq \max_{2\leq j\leq k}\left(Q^{k+1}|X^{(0)}|, Q^{k+1-j}|\Delta^{(j)}|\right) \ \text{for } j \geq 2 \ ,
\end{aligned} \tag{3.2}$$

with the additional constraints $\delta(X)^{(2)} \geq Q\delta(X)^{(0)}$ and $\delta(X)^{(k)} \geq Q\delta(X)^{(k-1)}$ for $k \geq 3$ are imposed on the truncation errors. The chiral expansion parameter Q is

$$Q = \max\left(\frac{p}{\Lambda_b}, \frac{m_\pi}{\Lambda_b}\right) \ . \tag{3.3}$$

In my calculations the breakdown scale of the chiral expansion Λ_b was choosen as $\Lambda_b = 600$ MeV based on the results from Refs [13, 14] with the physical pion mass m_π and the c.m.s. momentum p corresponding to the considered incoming-nucleon laboratory $E_{\rm lab}$.

3.1.3 The truncation errors with a given Bayesian model

Since the EKM approach does not provide a statistical interpretation of the alleged uncertainties, we apply also the Bayesian approach to estimate truncation error. The authors of Refs. [57, 15] developed the Bayesian method to calculate the posterior probability distribution of truncation errors in χEFT for the np total cross section at selected energies by applying the chiral NN potentials from Ref. [55]. Within the LENPIC project the Bayesian model of Ref. [15] was slightly modified to study truncation errors not only in NN but also in 3N scattering, [58]. The same Bayesian procedure was already used in Ref. [12].

This Bayesian procedure determining the truncation errors was based on rewriting Eq. (3.1) in terms of dimensionless expansion coefficients c_k in the form

$$\begin{aligned}
X &= X^{(0)} + \Delta X^{(2)} + \Delta X^{(3)} + \Delta X^{(4)} + \ldots + \Delta X^{(k)} + \ldots \\
&= X_{\rm ref}\left(c_0 + c_2 Q^2 + c_3 Q^3 + c_4 Q^4 + \ldots\right) \ ,
\end{aligned} \tag{3.4}$$

where $\Delta X^{(k)}$ are the same as in Eq. (3.2) and the dimensionless expansion coefficients c_k are

$$c_k = \frac{X^{(k)} - X^{(k-1)}}{X_{\rm ref} Q^k} \ . \tag{3.5}$$

The overall scale $X_{\rm ref}$ is

$$X_{\rm ref} = \begin{cases} \max\left(|X^{(0)}|, Q^{-2}|\Delta X^{(2)}|\right) & \text{for } k = 2 \ , \\ \max\left(|X^{(0)}|, Q^{-2}|\Delta X^{(2)}|, Q^{-3}|\Delta X^{(3)}|\right) & \text{for } k \geq 3 \ , \end{cases} \tag{3.6}$$

assuming that $\Delta X^{(i)}$ are known explicitly up to the $k = 3$. One can estimate the size of the truncation error at the k-th order of chiral expansion as $\delta X^{(k)}_{Bayes} \equiv X_{ref}\Delta$ where $\Delta \equiv \sum_{i=k+1}^{\infty} c_i Q^i \approx \sum_{i=k+1}^{k+h} c_i Q^i$ is distributed, given the knowledge of $\{c_{i\leq k}\}$ with a

posterior probability density function

$$\mathrm{pr}_h\left(\Delta \mid \{c_{i\leq k}\}\right) = \frac{\int_0^\infty d\bar{c}\ \mathrm{pr}_h\left(\Delta \mid \bar{c}\right)\mathrm{pr}(\bar{c})\prod_{i\in A}\mathrm{pr}(c_i \mid \bar{c})}{\int_0^\infty d\bar{c}\ \mathrm{pr}(\bar{c})\prod_{i\in A}\mathrm{pr}(c_i \mid \bar{c})}\ . \tag{3.7}$$

Here the prior probability density function $\mathrm{pr}(c_i \mid \bar{c})$ is taken in form of a Gaussian $\mathrm{N}(0,\bar{c}^2)$ function and $\mathrm{pr}(\bar{c})$ is a log-uniform distribution in range $(\bar{c}_<, \bar{c}_>)$. Set A is defined as $A = \{n \in \mathrm{N}_0 \mid \mathrm{n} \leq \mathrm{k}\ \wedge\ \mathrm{n} \neq 1 \wedge \mathrm{n} \neq \mathrm{m}\}$, $m \in \{0, 2, 3\}$ and

$$\mathrm{pr}_h(\Delta \mid \bar{c}) \equiv \left[\prod_{i=k+1}^{k+h}\int_\infty^\infty dc_i \mathrm{pr}(c_i \mid \bar{c})\right]\delta\left[\Delta - \sum_{j=k+1}^{k+h} c_j Q^j\right]\ , \tag{3.8}$$

with h being the number of the chiral orders above k which contributes to the truncation error. Resulting $\mathrm{pr}_h(\Delta \mid \{c_{i\leq k}\})$ is symmetric about $\Delta = 0$ thus one can find the degree-of-belief (DoB) interval $(-d_k^{(p)}, d_k^{(p)})$ at the probability p, as an inversion problem from the numerical integration

$$p = \int_{-d_k^{(p)}}^{d_k^{(p)}} \mathrm{pr}_h(\Delta \mid \{c_{i\leq k}\})d\Delta \tag{3.9}$$

and thus find the truncation error $\delta X_{Bayes}^{(k)} = X_{ref} d_k^{(p)}$.

In following we use $h = 10$, $\bar{c}_< = 0.5$, $\bar{c}_> = 10$, $\Lambda_b = 650$ MeV and $M_\pi^{\mathrm{eff}} = 200$ MeV. The two latter quantities enter the expansion parameter $Q = max\left(\frac{p}{\Lambda_b}, \frac{M_\pi^{\mathrm{eff}}}{\Lambda_b}\right)$ with momentum scale p defined in Eq. (17) of Ref. [58] and reads as

$$p = \sqrt{\frac{A}{A+1} m E_{\mathrm{lab}}}\ , \tag{3.10}$$

where $A = 2$ for the deuteron, m is the nucleon mass $m = 2m_p m_n/(m_p + m_n) = 938.918$ MeV.

Finally, the detailed expression for $\mathrm{pr}_h\left(\Delta \mid \{c_{i\leq k}\}\right)$ at assumed priors[1] which was shown in Appendix A[2] of Ref. [58] takes the form

$$\begin{aligned}\mathrm{pr}_h\left(\Delta \mid \{c_{i\leq k}\}\right) = {} & \frac{1}{\sqrt{\pi\bar{q}^2 \boldsymbol{c_k^2}}}\left(\frac{\boldsymbol{c_k^2}}{\boldsymbol{c_k^2} + \Delta^2/\bar{q}^2}\right)^{k/2} \\ & \times \frac{\Gamma\left[\frac{k}{2}, \frac{1}{2c_>^2}\right]\left(\boldsymbol{c_k^2} + \frac{\Delta^2}{\bar{q}^2}\right) - \Gamma\left[\frac{k}{2}, \frac{1}{2c_<^2}\right]\left(\boldsymbol{c_k^2} + \frac{\Delta^2}{\bar{q}^2}\right)}{\Gamma\left[\frac{k-1}{2}, \frac{\boldsymbol{c_k^2}}{2c_>^2}\right] - \Gamma\left[\frac{k-1}{2}, \frac{\boldsymbol{c_k^2}}{2c_<^2}\right]}\end{aligned} \tag{3.11}$$

where $\bar{q}^2 \equiv \sum_{i=k+1}^{k+h} Q^{2i}$, $\boldsymbol{c_k^2} \equiv \sum_{i\in A} c_i^2$ and the incomplete gamma function is

$$\Gamma(s, x) = \int_x^\infty t^{s-1} e^{-t} \mathrm{dt}\ . \tag{3.12}$$

[1]Since, in general, the coefficients c_k are unknown *a priori*, they can be obtained from a random distribution (priors) with a characteristic size.

[2]The expression was first given in Appendix A of Ref. [15]

The choice of values of h, $\bar{c}_<$, $\bar{c}_<$ and Λ_b corresponds to the model $\bar{C}^{650}_{0.5-10}$ from Ref. [58].

3.2 Correlations among observables in reactions and bound states in 2N and 3N systems

In the second part of thesis (Chapter **??**) I focuse on looking for a set of observables which should (shouldn't) be taken into account while fixing the free parameters of the three-nucleon force. In general, to fix free parameters of the 3NFs various observables can be used. In the older models (like for the Tucson-Melbourne [74, 75, 76] or the UrbanaIX ones [77]) the ^{3}H binding energy and the density of the nuclear matter have been used.

As outlined in Introduction, in the case of the chiral models, besides the ^{3}H binding energy, the differential cross section for Nd elastic scattering at $E = 60$ MeV around its minimum has been used to fix free parameters of 3NF. However, the question of a possible correlation between the binding energy ^{3}H and the scattering cross section is still open. The answer is important since obviously using the strongly correlated observables to fix free parameters can bias results of such determination method. The study presented in this thesis allows me to answer this question and, in a systematic way, to point the correlated observables in the 3N system. However, the study of the correlations in the two-nucleon system is also interesting and can impact future procedures used to fix free parameters of the two-body force interaction. Also, a systematic study of the correlations between the parameters of the NN potential and two-nucleon observables can also be valuable. While there exist many experimental data at low energies most of them are the unpolarized cross sections or polarization observables with only one particle polarized in the initial state. Within this thesis, by testing the correlations between potential parameters and the 2N observables, I would like to check if there are observables which shows a strong sensitivity to a given single potential parameter. If this is a case such observable should be used to fix this specific parameter. This, in turn, will reduce the number of the remaining free parameters what would simplify the fitting procedure. Existence of such correlated observable-potential parameter pair could also motivate experimental groups to perform precise measurement of such observable, especially in case if the suitable experiment has not been performed yet. To the best of my knowledge, the studies proposed in thesis project have not been done yet. In the past, the study of the correlation, at a statistically significant level, has not been possible due to lack of enough big number of the potential models and data. Currently, this situation is changed. Using the OPE-Gaussian or the chiral SMS forces allow us to prepare many sets of the potential parameters and thus, after a procedure described in the previous subsection, obtain enough big number of predictions to analyze correlations and to draw a plausible conclusion. Some attempts to study correlations in few-nucleon sectors are given in papers [92], [93] and [94]. In Ref. [92] authors study, using the Monte-Carlo bootstrap analysis as a method to randomize *pp* and *np* scattering data, correlations between the ground states of the ^{2}H, ^{3}H and ^{4}He binding energies, focusing mainly on the Tijon line [95] (correlation between ^{3}H and ^{4}He binding energies), but not studying the scattering observables. In Ref. [93] the correlations between three- and four-nucleon observables have been studied within the pionless Effective Field Theory with the Resonating Group Method. Because this method can be applied only to processes at very low energies authors focus on study bound state properties and the ^{3}H-neutron s-wave scattering length, finding the latter correlated with the ^{3}He binding energy. A.

Kievsky *et al.*, [94] studied some correlations between low-energy bound observables in the two- and three-nucleon system, the triton binding energy, and extending this to study some features of the light nuclei and beyond up to the nuclear matter and neutron star properties. Using a simple model of "Leading-order Effective Field Theory inspired potential" they found evidence of the connection between few- and many observables. Note, none of these works focuses on study correlations in the context of fixing 3NF parameters.

In practice, when all observables and potential parameters are collected, I calculate the standard sample correlation coefficients $r(X, Y)$

$$r(X,Y) = \frac{\sum_{i=1}^{n} \left(x_i - \bar{X}\right)\left(y_i - \bar{Y}\right)}{\sqrt{\sum_{i=1}^{n} \left(x_i - \bar{X}\right)^2 \sum_{i=1} \left(y_i - \bar{Y}\right)^2}} \,, \tag{3.13}$$

where X and Y stand for chosen observables or parameters and index "i" runs over sets of $n = 50$ versions of potentials. $\bar{X}$ and $\bar{Y}$ denote averages $\bar{X} = \sum_{i=1}^{n} x_i$, $\bar{Y} = \sum_{i=1}^{n} y_i$. Results for sample correlation coefficients and the conclusions on mutual relations and correlations of observables and/or potential parameters are presented in Chapter **??**.

Chapter 4

Theoretical formalism and numerical realization

All results in this work have been obtained in momentum space by resorting to partial-wave decomposition (PWD) what is convenient for calculations in the framework of the Faddeev equations. We use the non-relativistic formalism, neglect the Coulomb force and 3N interaction.

4.1 2N bound state

The Hamiltonian of two-nucleon systems can be written in general form

$$H^{(2)} = H_0^{(2)} + V_{\rm 2N} \ , \tag{4.1}$$

where $H_0^{(2)}$ is the kinetic energy of two nucleons and $V_{\rm 2N}^{(2)}$ is the NN potential. The kinetic energy of the two-particle system is

$$H_0^{(2)} = \frac{\vec{p}_1^{\,2}}{2m_1} + \frac{\vec{p}_2^{\,2}}{2m_2} = \frac{\vec{p}^{\,2}}{2\mu} + \frac{\vec{\mathcal{P}}^{\,2}}{2M} \ , \tag{4.2}$$

where $\mu = \frac{m_1 m_2}{m_1+m_2}$ is the reduced nucleon mass and $M = m_1 + m_2$. Using the average nucleon mass $m_1 = m_2 = m = \frac{2m_p m_n}{m_p+m_n}$ we have the relative momentum $\vec{p} = \frac{m_1\vec{p}_2 - m_2\vec{p}_1}{m_1+m_2} = \frac{1}{2}\left(\vec{p}_2 - \vec{p}_1\right)$ and $\vec{\mathcal{P}} = \vec{p}_1 + \vec{p}_2$ the total momentum for two nucleons.

The deuteron bound wave function $|\Psi_d\rangle$ is a solution of the time-independent Schrödinger equation

$$\left(H_0^{(2)} + V_{\rm 2N}\right)|\Psi_{\rm d}\rangle = E_d\,|\Psi_{\rm d}\rangle \ , \tag{4.3}$$

where $E_d < 0$. Using Eq. (4.2) and assuming that $V_{\rm 2N}$ depends only on the relative degrees of freedom leads to two separated equations

$$\frac{\vec{p}^{\,2}}{m}\,\langle\vec{p}|\Psi_d\rangle + \int_0^\infty {\rm d}\vec{p}\,'\,\langle\vec{p}\,'|V_{\rm 2N}|\vec{p}\rangle\,\langle\vec{p}\,'\big|\Psi_d\rangle = (E_d - E_{\rm c.m.})\,\langle\vec{p}|\Psi_d\rangle \ , \tag{4.4}$$

and

$$\frac{\vec{\mathcal{P}}^{\,2}}{2m}\left\langle\vec{\mathcal{P}}|\Psi_d\right\rangle = E_{\rm c.m.}\left\langle\vec{\mathcal{P}}|\Psi_d\right\rangle \ . \tag{4.5}$$

Since the total momentum of the system is conserved, the relative energy of the center of mass between two nucleons, $E_{\mathrm{c.m.}}$, equals zero (deuteron is at rest) and the equation (4.5), which describes the free motion of a particle with mass M, is omitted.

We use the momentum partial-wave representation

$$|p\alpha_2\rangle \equiv |p(ls)jm_j\rangle\,|tm_t\rangle \ , \tag{4.6}$$

where $p \equiv |\vec{p}|$ is the magnitude of the relative momentum, and α_2 is a set of discrete quantum numbers describing 2N system $|\alpha_2\rangle \equiv |(ls)jm_j\rangle\,|tm_t\rangle$, where l, s, j, and t denote the orbital angular momentum, total spin, total angular momentum, and total isospin of 2N system, respectively. Further m_j (m_t) are the projections of j (t) onto quantization axis. The coupling of above-mentioned quantum numbers is given by

$$\begin{aligned}
|p(ls)jm_j\rangle &= \sum_{m_l} c(lsj; m_l, m_j - m_l, m_j)\,|plm_l\rangle\,|sm_j - m_l\rangle \ , \\
|sm_s\rangle &= \sum_{m_1=-1/2}^{1/2} C\left(\frac{1}{2},\frac{1}{2},s; m_1, m_s - m_1, m_s\right)\left|\frac{1}{2}m_1\right\rangle\left|\frac{1}{2}m_s - m_1\right\rangle \ , \\
|tm_t\rangle &= \sum_{\nu=-1/2}^{1/2} C\left(\frac{1}{2},\frac{1}{2},t; \nu, m_s - \nu, m_t\right)\left|\frac{1}{2}\nu\right\rangle\left|\frac{1}{2}m_t - \nu\right\rangle \ ,
\end{aligned} \tag{4.7}$$

where m_l is the projection of the orbital angular momentum. Further, spin states $|sm_s\rangle$ correspond to 2N spin states with the total spin 0 or 1; $C(j_1, j_2, j; m_1, m_2, m)$ denote the Clebsch-Gordan coefficients. Similarly, $|tm_t\rangle$ is the isospin state. We assume for individual particles the isospin projection $\nu = \frac{1}{2}$ for proton and $\nu = -\frac{1}{2}$ for neutron.

The 2N states are antisymmetric as for a system of two identical fermions, which leads to one more constraint on quantum numbers l, s and t

$$(-1)^{l+s+t} = -1 \ . \tag{4.8}$$

The partial-wave states (4.6) fulfills

$$\left\langle \vec{p}\,'|plm_l\right\rangle = \frac{\delta(p-p')}{pp'} Y_{lm_l}(\theta,\phi) \ , \tag{4.9}$$

where $Y_{lm_l}(\theta,\phi)$ denotes the spherical harmonic function with angles θ, ϕ pointing direction of momentum $\vec{p}$ [96]. The completeness relation for $|p\alpha_2\rangle$ states is expressed as

$$\sum_{\alpha_2} \int_0^\infty \mathrm{d}pp^2\,|p\alpha_2\rangle\,\langle p\alpha_2| = \mathbb{1} \ . \tag{4.10}$$

The only two deuteron components ${}^3S_1$- and ${}^3D_1$ (we use the standard notation ${}^{2s+1}l_j$), corresponds to $l = 0$ and $l = 2$, respectively, with $s = j = 1$ and $t = m_t = 0$. This leads to two coupled equations

$$\frac{p^2}{m}\psi_l(p) + \sum_{l',l=0}^{2} \int_0^\infty dp'p'^2\,\langle pl|V_{\mathrm{2N}}|p'l'\rangle\,\psi_{l'}(p') = E_d\psi_l(p) \ , \tag{4.11}$$

	N^2LO	N^3LO	N^4LO	N^4LO^+	OPEG	Exp. [97]
E_d [MeV]	-2.1999 $\pm$0.0041	-2.2233 $\pm$0.0024	-2.2233 $\pm$0.00099	-2.2233 $\pm$0.0012	-2.2225 $\pm$0.00001	-2.2246 $\pm$0.0092
$P(^3S_1)$ [%]	95.3665 $\pm$0.0041	95.3034 $\pm$0.0024	95.4633 $\pm$0.00099	95.4114 $\pm$0.0012	94.6987 $\pm$0.0412	—

Table 4.1: The deuteron binding energy E_d with the statistical uncertainty (see text in Chapter 3.1.1) obtained with various NN interactions.

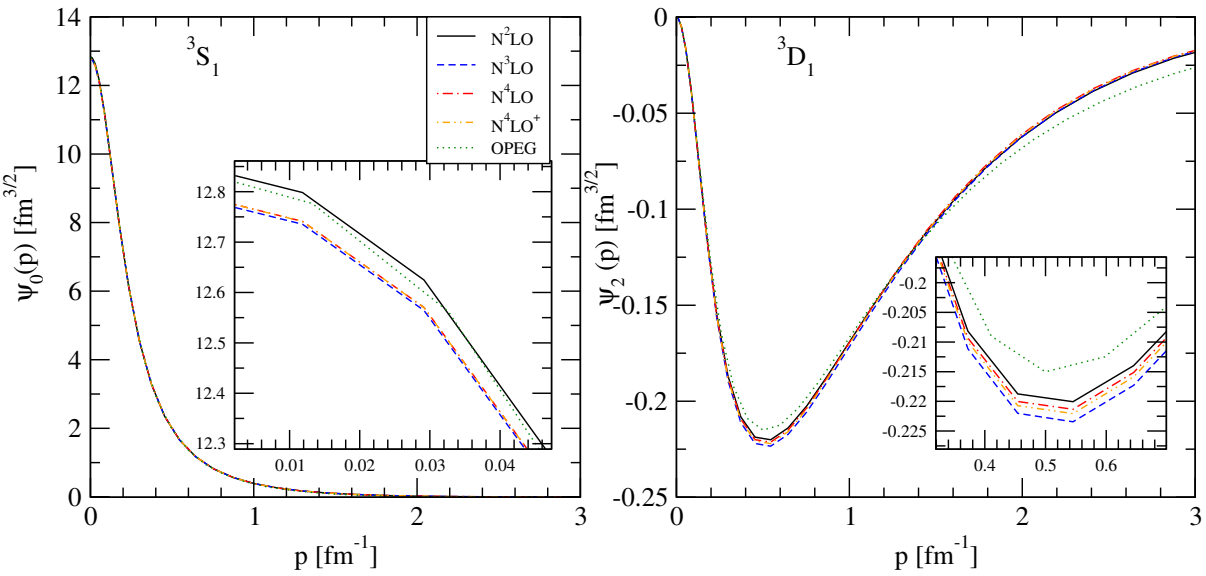

Figure 4.1: The deuteron wave functions in momentum $\Psi_l(p)$ space. The $^3S_1$ and the $^3D_1$ components are shown in the left and right columns, respectively. The black solid, blue dashed, red dashed-dotted, orange dashed-dot-dotted and green dotted curves are for the chiral N^2LO, N^3LO, N^4LO, N^4LO^+ and the OPEG potentials, respectively.

for the partial-wave components of the deuteron wave function $\psi_l(p) = \langle pl|\psi_d\rangle = \langle p(l1)1m_d|\,\langle 00|\psi_d\rangle$ The integral (4.11) can be discretized using the Gaussian quadrature with Gaussian points and weights (p_j, w_j) with $j = 1, 2, \ldots, N_p$ distributed in the finite interval $(0, \bar{p})$, where the upper limit of the integration, $\bar{p}$ has to be adjusted to the used NN potential V_{2N}. Than, Eq. (4.11) expresses as

$$\frac{p_i^2}{m}\psi_l(p_i) + \sum_{l'=0}^{2}\sum_{j=1}^{N_p} w_j p_j'^2 \,\langle p_i l|V_{2N}|p_j l'\rangle\, \psi_{l'}(p_j) = E_d \psi_l(p_i)\ . \tag{4.12}$$

We solve the resulting an eigenvalue problem, using the FORTRAN code together with the LAPACK library and compute the deuteron wave function and the deuteron binding energy, E_d. The deuteron binding energy computed with the chiral SMS potentials at various chiral orders with cutoff $\Lambda = 450$ MeV and with the OPE-Gaussian force is given in Table 4.1. In the final step the deuteron wave functions $\psi_0(p)$ and $\psi_2(p)$ require normalization via

$$\int_0^\infty dp p^2 \left(\psi_0^2(p) + \psi_2^2(p)\right) = 1\ . \tag{4.13}$$

In Figure 4.1 I show the ${}^3S_1$- and ${}^3D_1$-states obtained by using the chiral N^{2}LO, N^{3}LO, N^{4}LO, N^{4}LO$^+$ SMS forces and the OPE-Gaussian potential. It can be seen that all predictions almost coincide with each other. The magnitude of ${}^3S_1$-state is nearly 70 times bigger than in ${}^3D_1$-state. The corresponding ${}^3S_1$-component probability is given in the bottom row of Table 4.1.

4.2 2N scattering

In this chapter I introduce the essential components of 2N scattering calculations. I start with a discussion of the Lippman-Schwinger equation for the scattering state in momentum space. Solving it in terms of the transition matrix (t-matrix) by realizing its PWD one gets the half-the-energy-shell amplitude (half-shell amplitude). Next, I obtain K-matrix, which in turn, is related to the scattering matrix S-matrix. S-matrix can be further expressed in terms of a linear combination of Wolfenstein parameters that allowed us to compute observables, e.g. the cross-section and various polarization observables at various energies.

4.2.1 The Lippman-Schwinger equation in PWD

The scattering state $|\Psi_{\vec{p}}\rangle$ of two particles in momentum space, fulfils the time-independent Schrödinger equation

$$(H_0 + V_{2\mathrm{N}})\,|\Psi_{\vec{p}}\rangle = E\,|\Psi_{\vec{p}}\rangle \ , \tag{4.14}$$

with $E > 0$. Its solution fulfils the Lippman-Schwinger equation

$$|\Psi_{\vec{p}}\rangle = |\Psi_0\rangle + \frac{1}{E - H_0 \pm i\varepsilon} V_{2\mathrm{N}}\,|\Psi_{\vec{p}}\rangle \ , \tag{4.15}$$

with $\varepsilon \to 0^+$. If we write down (4.15) in coordinate representation, we will get two parts of the solution — a spherical outgoing wave ($+i\varepsilon$) or a plane incoming wave ($-i\varepsilon$) [1], see Refs. [98, 99] for more details. The state $|\Psi_0\rangle$ is momentum eigenstate

$$|\Psi_0\rangle \equiv |\vec{p}\rangle \ \text{ with } \frac{\vec{p}^{\,2}}{2\mu} = E \ , \tag{4.16}$$

where $\vec{p}$ is the relative momentum of the two nucleons and E depends on the incoming nucleon energy in the laboratory reference frame [2]. The solution of Eq. (4.15) can be denoted as $|\Psi_{\vec{p}}\rangle = |\vec{p}\rangle^+$.

Eq. (4.15) can be rewritten as

$$|\vec{p}\rangle^+ = |\vec{p}\rangle + \tilde{G}_0(E + i\varepsilon) V_{2\mathrm{N}}\,|\vec{p}\rangle^+ \ , \tag{4.17}$$

where $V \equiv V_{2\mathrm{N}}$ and the free propagator

$$\tilde{G}_0(E) \equiv \frac{1}{E - H_0} \ . \tag{4.18}$$

[1] "$-i\varepsilon$"-states appear, for example, in the photodisintegration process ($\gamma + {}^2\mathrm{H} \to n + p$).

[2] Given E_{lab} and assuming that $m_p = m_n = m$, each nucleon in the c.m.s. has a relative momentum which refers to an unknown $E \equiv E_{\mathrm{cm}} = \frac{\vec{p}^{\,2}}{m}$. In turn, $E = E_{\mathrm{lab}} - \frac{\vec{p}^{\,2}}{2(2m)} = \frac{1}{2} E_{\mathrm{lab}}$.

Using the definition of the transition operator (t-matrix)

$$V\,|\vec{p}\rangle^{+} = t^{+}\,|\vec{p}\rangle \ , \tag{4.19}$$

and substituting it into Eq. (4.17) we find

$$V\,|\vec{p}\rangle^{+} = V\,|\vec{p}\rangle + V\tilde{G}_0(E+i\varepsilon)V\,|\vec{p}\rangle^{+} \ , \tag{4.20}$$

and thus

$$t^{+}\,|\vec{p}\rangle = V\,|\vec{p}\rangle + V\tilde{G}_0(E+i\varepsilon)t^{+}\,|\vec{p}\rangle \ . \tag{4.21}$$

The latter equation is the form of the Lippman-Schwinger equation for the operator t^{+}

$$t^{+} = V + V\tilde{G}_0(E+i\varepsilon)t^{+} \ . \tag{4.22}$$

Note that in general case Eq. (4.22) can be iterated for scattering on V

$$t = V + V\tilde{G}_0V + V\tilde{G}_0V\tilde{G}_0V + V\tilde{G}_0V\tilde{G}_0V\tilde{G}_0V + \dots \ , \tag{4.23}$$

this is so-called von Neumann series. Finally one can express $|\vec{p}\rangle^{+}$ through the t-matrix

$$|\vec{p}\rangle^{+} = |\vec{p}\rangle + \tilde{G}_0(E+i\varepsilon)t(E+i\varepsilon)\,|\vec{p}\rangle \tag{4.24}$$

Considering the t-matrix for general states $\left|\vec{p}\,'\right\rangle$, $|\vec{p}\rangle$, which obeys the Lippman-Schwinger equation (4.15), we get the off-the-energy-shell amplitude [98]

$$\begin{aligned}\left\langle\vec{p}\,'\right|t(E+i\varepsilon)\left|\vec{p}\right\rangle &= \left\langle\vec{p}\,'\right|V(E+i\varepsilon)\left|\vec{p}\right\rangle \\ &+ \lim_{\varepsilon\to 0^{+}}\int_0^{\infty}\mathrm{d}\vec{p}\,''\left\langle\vec{p}\,''\right|V(E+i\varepsilon)\left|\vec{p}\right\rangle\frac{\left\langle\vec{p}\,'\right|t\left|\vec{p}\right\rangle}{E_{p'}+i\varepsilon-E_{p''}} \ ,\end{aligned} \tag{4.25}$$

where $E_{p'}=\frac{|\vec{p}\,'|^2}{m}$ and $E_{p''}=\frac{|\vec{p}\,''|^2}{m}$. In a similar manner as has been done for the deuteron, PWD projection of Eq. (4.25) onto the same complete set of basis state (4.6) and using the upper limit for the p'' integration, $\bar{p}$, results in

$$\begin{aligned}\langle p'\alpha_2'|t|p\alpha_2\rangle &= \langle p'\alpha_2'|V|p\alpha_2\rangle + \\ &\sum_{l''=j-1,j+1}\lim_{\varepsilon\to 0^{+}}\int_0^{\bar{p}}\mathrm{d}p''\frac{p''^2\,\langle p''\alpha_2'|V|\vec{p}\rangle\,\langle p'\alpha_2'|t|p\alpha_2\rangle}{E_{p'}-E_{p''}+i\varepsilon} \ ,\end{aligned} \tag{4.26}$$

The t-matrix at $E=\frac{p^2}{m}$ is related to the K-matrix [98] via

$$t = (1+2i\pi\mu pK)^{-1}K \ . \tag{4.27}$$

and to the S-matrix via

$$S = (1+2i\pi\mu pK)^{-1}(1-2i\pi\mu pK)^{-1} \ . \tag{4.28}$$

which is used to get phase-shifts.

4.2.2 2N scattering observables

Studying the scattering of particles with spin 1/2 allows one to carry out much more diverse measurements than only cross sections. Experiments can be made for different polarization of the beam, target and/or outgoing particles, polarized individually or simultaneously. As a result, there are $16 \times 16 = 256$ of various experiments, but due to the parity conservation and the time- reversal symmetry, the number of independent experiments is reduced up to 11 *np*- and 9 *pp*-measurements [98]. The general scattering amplitude can be written as M-matrix and its representation is

$$\begin{aligned} M = a + c\,(\vec{\sigma}_1 + \vec{\sigma}_2)\,\hat{N} + m\left(\vec{\sigma}_1\hat{N}\right)\left(\vec{\sigma}_2\hat{N}\right) + (g+h)\left(\vec{\sigma}_1\hat{P}\right)\left(\vec{\sigma}_2\hat{P}\right) \\ + (g-h)\left(\vec{\sigma}_1\hat{K}\right)\left(\vec{\sigma}_2\hat{K}\right)\ , \end{aligned} \tag{4.29}$$

where a, m, c, g and h are the Wolfenstein parameters and

$$\hat{K} \equiv \frac{\vec{p}\,' - \vec{p}}{|\vec{p}\,' - \vec{p}|}\ ,\ \hat{P} \equiv \frac{\vec{p}\,' + \vec{p}}{|\vec{p}\,' + \vec{p}|}\ ,\ \hat{N} \equiv \frac{\vec{p}\,' \times \vec{p}}{|\vec{p} \times \vec{p}\,'|}\ . \tag{4.30}$$

Since the S -matrix contains full dynamic information, then decomposing it on partial-waves basis $S^{js}_{l'l}$-matrix elements and taking it on-the-energy-shell allows to calculate the partial-wave elements of M, see Ref. [98],

$$\begin{aligned} M^{st}_{m'_s m_s} = \frac{1}{ip}\sum_{jl'l} C\,(l', s, j; m_s - m'_s, m'_s, m_s)\,Y_{l'(m'_s - m_s)}(\theta, \phi) \\ \times\, i^{l-l'}\left(S^{js}_{l'l} - \delta_{l'l}\right) C\,(l, s, j; 0, m_s, m_s)\,\sqrt{\pi(2l+1)}\left[1 - (-1)^{l+s+t}\right]\ . \end{aligned} \tag{4.31}$$

The partial-wave $S^{js}_{l'l}$-matrix element is nothing else but $S^{js}_{l'l} \equiv \langle l'sj|S|lsj\rangle$.

In the uncoupled case ($l = l'$) the S-matrix can be parametrized by one phase shift

$$S^{js}_{ll} = e^{2i\delta_l}\ . \tag{4.32}$$

For the coupled channels (for which the nuclear force allows for changes of angular momentum) the S-matrix is 2×2 unitary and symmetric. According to the Stapp parametrisaton [100] it can be written as

$$S = \begin{pmatrix} \cos(2\varepsilon)\exp(2i\delta_1) & i\sin(2\varepsilon)\exp(i(\delta_1+\delta_2)) \\ i\sin(2\varepsilon)\exp(i(\delta_1+\delta_2)) & \cos(2\varepsilon)\exp(2i\delta_2) \end{pmatrix}\ , \tag{4.33}$$

where δ_1, δ_2 are phase shifts and ε is a mixing parameter.

Using the M-matrix [98], the resulting spin averaged differential cross section is given by

$$\frac{d\sigma}{d\Omega} = \frac{1}{4}\mathrm{Tr}\{MM^\dagger\}\ . \tag{4.34}$$

The polarization of one of the two particles is defined as

$$P = \frac{\mathrm{Tr}\{MM^\dagger\vec{\sigma}\}}{\mathrm{Tr}\{MM^\dagger\}} = \frac{8\mathrm{Re}\{c^*(a+m)\}}{\mathrm{Tr}\{MM^\dagger\}}\hat{N}\ , \tag{4.35}$$

where $\vec{\sigma}$ can be either $\vec{\sigma}_1$ or $\vec{\sigma}_2$.

The remaining 2N scattering spin observables expresses as

$$
\begin{aligned}
D &= \frac{\mathrm{Tr}\{M(\vec{\sigma}\cdot\hat{N})M^{\dagger}(\vec{\sigma}\cdot\hat{N})\}}{\mathrm{Tr}\{MM^{\dagger}\}}\,, \\
R &= \frac{\mathrm{Tr}\{M(\vec{\sigma}\hat{N}\times\hat{p})M^{\dagger}(\vec{\sigma}\cdot\hat{K})\}}{\mathrm{Tr}\{MM^{\dagger}\}}\,, \\
R' &= \frac{\mathrm{Tr}\{M(\vec{\sigma}\hat{N}\times\hat{p})M^{\dagger}(\vec{\sigma}\cdot\hat{P})\}}{\mathrm{Tr}\{MM^{\dagger}\}}\,, \\
A &= \frac{\mathrm{Tr}\{M(\vec{\sigma}\cdot\hat{p})M^{\dagger}(\vec{\sigma}\cdot\hat{K})\}}{\mathrm{Tr}\{MM^{\dagger}\}}\,, \\
A' &= \frac{\mathrm{Tr}\{M(\vec{\sigma}\cdot\hat{p})M^{\dagger}(\vec{\sigma}\cdot\hat{P})\}}{\mathrm{Tr}\{MM^{\dagger}\}}\,,
\end{aligned}
\tag{4.36}
$$

where $\hat{p} = (\sin\theta\cos\phi, \sin\theta\sin\phi, \cos\theta)$. The observable D determines the change of polarization with respect to normal direction, the depolarisation observables R, R', A, and A' determine the four possible linear combinations referring to beam and target spin polarization in scattering plane.

In the case of two polarised particles we find the spin-correlation coefficients, e.g.

$$
C_{NN} = \frac{\mathrm{Tr}\{MM^{\dagger}\vec{\sigma}_1\cdot\hat{N}\vec{\sigma}_2\cdot\hat{N}\}}{\mathrm{Tr}\{MM^{\dagger}\}}\,. \tag{4.37}
$$

More detailed information about the 2N scattering observables and the partial-wave decomposition can be found in Ref. [98].

4.3 The Faddeev equation

Theoretical investigations of Nd scattering can be performed within the Faddeev equations. This is one of the standard techniques to investigate 3N reactions and has been described in detail many times, see, e.g. Refs. [1, 2, 98]. In following I will just briefly describe the key points of the formalism and its practical implementation.

In case of 3N system it is convenient to use the relative ($\vec{p}$ and $\vec{q}$) momenta and the total 3N momentum, $\vec{\mathcal{P}}$ represented by individual nucleon momenta $\vec{k}_i$, $i \in \{1,2,3\}$

$$
\begin{aligned}
\vec{p} &= \frac{1}{2}\left(\vec{k}_2 - \vec{k}_3\right)\,, \\
\vec{q} &= \frac{2}{3}\left(\vec{k}_1 - \frac{1}{2}\left(\vec{k}_2 + \vec{k}_3\right)\right)\,, \\
\vec{\mathcal{P}} &= \vec{k}_1 + \vec{k}_2 + \vec{k}_3\,.
\end{aligned}
\tag{4.38}
$$

The Jacobi momentum $\vec{p}$ is a relative momentum of nucleons 2 and 3 and the Jacobi momentum $\vec{q}$ is the momentum of nucleon 1 with respect to the center of mass of the 2-3 subsystem. The definition 4.38 can be extended to a more general case where the Jacobi momenta $\vec{p}_i$, $\vec{q}_i$ are used, see Figure 4.2. We are working in 3N center of mass system what allows us to deal with 2 instead of 3 independent momenta, $\vec{\mathcal{P}} = \vec{0}$.

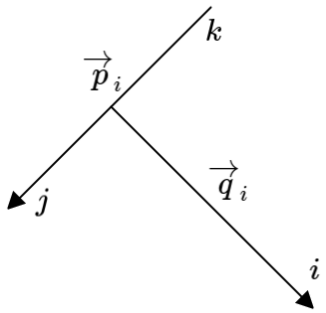

Figure 4.2: Jacobi momenta $\vec{p}_i$ and $\vec{q}_i$ depending on suitable permutations.

The full 3N Hamiltonian reads

$$H = H_0 + V_{23} + V_{13} + V_{12} + V_{123} \ , \tag{4.39}$$

where $H_0 = \frac{\vec{p}^2}{m} + \frac{3}{4}\frac{\vec{q}^2}{m}$ is the free 3N Hamiltonian in the c.m. frame in terms of the Jacobi momenta, V_{ij} denotes the NN potential acting between nucleons i and j, and V_{123} is the 3N potential, which can be always splitted to potential $V^{(i)}$ symmetric under the exchange of nucleons j and k:

$$V_{123} = V_4^{(1)} + V_4^{(2)} + V_4^{(3)} \ , \tag{4.40}$$

where $V_4^{(1)}$ is symmetric under the exchange of nucleons 2 and 3. In the case of three identical particles the totally antisymmetric state $|\Psi\rangle$ of three nucleons is given by

$$|\Psi\rangle = |\psi_1\rangle + |\psi_2\rangle + |\psi_3\rangle = (1+P)\,|\psi_1\rangle \ , \tag{4.41}$$

where the permutation operator $P \equiv P_{12}P_{23} + P_{13}P_{23}$ is built from transmutations P_{ij}, which exchange particles i and j and $|\psi_1\rangle$ the Faddeev component of $|\Psi\rangle$. For example, the three-nucleon bound state $|\Psi_b\rangle$ fulfills the eigenvalue equation [68]

$$|\psi_1\rangle = G_0 t P\,|\psi_1\rangle \ , \tag{4.42}$$

where the two-nucleon t-operator obtaining by Eq. (4.22) acts now in the 3N space and G_0 is the free 3N propagator. For the 3N bound states, the energy argument of G_0 plays the role of the binding energy.

The transition amplitude U for the elastic Nd scattering is calculated prior to computing 3N scattering observables. Its matrix elements between the initial Nd $|\phi\rangle$ and final Nd $|\phi'\rangle$ scattering state are given by [2]

$$\langle\phi'|U|\phi\rangle = \left\langle\phi'|PG_0^{-1}|\phi\right\rangle + \langle\phi'|PT|\phi\rangle \ . \tag{4.43}$$

For the deuteron breakup reaction the transition amplitude U_0 fulfils

$$\langle\phi_0'|U_0|\phi_0\rangle = \langle\phi_0'|(1+P)T|\phi_0\rangle \ , \tag{4.44}$$

where $|\phi_0'\rangle$ carries the information about the final free three-nucleon breakup channel.

The Faddeev equation for the auxiliary state $T\,|\phi\rangle$ for which nucleons interact via a

NN interaction V entering a t-matrix and a 3NF V_4 expressed as

$$\begin{aligned} T\,|\phi\rangle &= tP\,|\phi\rangle + tPG_0T\,|\phi\rangle + (1+tG_0)V_4^{(1)}(1+P)\,|\phi\rangle \\ &\quad + (1+tG_0)V_4^{(1)}(1+P)T\,|\phi\rangle \ , \end{aligned} \tag{4.45}$$

where the initial state $|\phi\rangle = |\varphi_d m_d\rangle\,|\vec{q}_0 m_N\rangle$ is composed of the deuteron wave function $|\varphi_d\rangle$ and a relative momentum eigenstate of the projectile nucleon, $|\vec{q}_0\rangle$, with corresponding the spin quantum numbers m_d and m_N, respectively. This equation is the key equation for the nucleon-deuteron scattering and also the basis of predictions shown in this thesis. Neglecting the 3NF, Eq. (4.45) reduces to

$$T\,|\phi\rangle = tP\,|\phi\rangle + tPG_0T\,|\phi\rangle \ . \tag{4.46}$$

Now one can introduce momentum basis states for the 3N systems. We perform PWD of three-nucleons operators in $|pq\alpha\rangle$ basis

$$\begin{aligned} &|pq\alpha\rangle \equiv \left|pq\,(ls)\,j\left(\lambda\frac{1}{2}\right)I\,(jI)\,JM_J\right\rangle \left|\left(t\frac{1}{2}\right)TM_T\right\rangle = \\ &\sum_{m_j} C(jIJ;m_j,M_J-m_j)\,|p(ls)JM_J\rangle \left|q\left(\lambda\frac{1}{2}\right)IM_J-m_j\right\rangle \\ &\sum_{m_t} C(t\frac{1}{2}T;m_t,M_T-m_t)\,|tm_t\rangle \left|\frac{1}{2}M_T-m_t\right\rangle \ . \end{aligned} \tag{4.47}$$

Here, l, s, j, and t denotes the orbital angular momentum, total spin, total angular momentum, and total isospin of the 2-3 c.m.s. subsystem, respectively, with $p=|\vec{p}|$ and $q=|\vec{q}|$ being the magnitudes of the Jacobi momenta $\vec{p}$. Next, the motion of nucleon 1 with respect to 2-3 c.m.s. subsystem is given in terms of the orbital momentum, λ is coupled with its spin $\frac{1}{2}$ to give the total angular momentum of nucleon 1, I. Further, j is coupled with I to give the total angular momentum of the 3N system, J, with its projection M_J on the quantization axis $\hat{z}$. Finally, T and M_T are the total 3N isospin and its projection. T arises from coupling of 2N isospin $t=0$, 1 and the isospin $\frac{1}{2}$ of the nucleon 1. The $|pq\alpha\rangle$ basis is orthonormalized as

$$\langle p'q'\alpha'|pq\alpha\rangle = \frac{\delta(q'-q)}{qq'}\frac{\delta(p'-p)}{pp'}\delta_{\alpha\alpha'} \ , \tag{4.48}$$

satisfies conditions of antisymmetrization of 2-3 subsystem by constraint $(-1)^{l+s+t}=-1$ and its normalization is

$$\sum_\alpha \int_0^\infty dpp^2 \int_0^\infty dqq^2\,|pq\alpha\rangle\,\langle pq\alpha| = \mathbb{1} \ . \tag{4.49}$$

The first step of our way of the Faddeev equation (4.46) is projection on the basis

states of Eq. (4.47) [2, 98]

$$\begin{aligned}\langle pq\alpha|T|\phi\rangle = \langle pq\alpha|tP|\phi\rangle + \sum_{\alpha'}\int\limits_0^\infty dp'p'^2\int\limits_0^\infty dq'q'^2\sum_{\alpha''}\int\limits_0^\infty dp''p''^2\int\limits_0^\infty dq''q''^2 \\ \langle pq\alpha|t|p'q'\alpha'\rangle\,\langle p'q'\alpha'|P|p''q''\alpha''\rangle\,\langle p''q''\alpha''|G_0T|\phi\rangle\ .\end{aligned} \tag{4.50}$$

The t-matrix is diagonal in the quantum numbers of the nucleon 1

$$\begin{aligned}\langle pq\alpha|t(E)|p'q'\alpha'\rangle =& \frac{\delta(q-q')}{qq'}\delta_{\lambda\lambda'}\delta_{ss'}\delta_{tt'}\delta_{jj'}\delta_{II'}\delta_{JJ'}\delta_{m_Jm_{J'}}\delta_{TT'}\delta_{m_Tm_{T'}} \\ & \tilde{t}_{\tilde{\alpha}_2\tilde{\alpha}'_2}\left(p,p',E-\frac{3}{4}\frac{\vec{q}^{\,2}}{m}\right)\ ,\end{aligned} \tag{4.51}$$

where $\tilde{t}$ denotes the NN t-matrix and $\tilde{\alpha}_2$ contains the information about $lsjt$ components.

Assuming that $T=T'=1/2$, the two-nucleon t-matrix in the two-nucleon subsystem takes the form [101, 102]

$$\left\langle\left(t\frac{1}{2}\right)T|t|\left(t'\frac{1}{2}\right)T'\right\rangle = \delta_{tt'}\delta_{TT'}\delta_{T1/2}\left[\delta_{t0}t_{np}^{t=0}+\delta_{t1}\left(\frac{2}{3}t_{nn}^{t=1}+\frac{1}{3}t_{np}^{t=1}\right)\right]\ . \tag{4.52}$$

For the elastic scattering the isospin $T=\frac{3}{2}$ components are negligible.

Among various expressions for $\langle p'q'a^\alpha|P|pq\alpha\rangle$ we use [2]

$$\langle p'q'\alpha'|P|pq\alpha\rangle = \int\limits_{-1}^{1}dx\frac{\delta(p'-\pi_1)}{p''^{l'+2}}\frac{\delta(p-\pi_2)}{p'^{l+2}}G_{\alpha'\alpha}(q'qx)\ , \tag{4.53}$$

where

$$\pi_1=\sqrt{q^2+\frac{1}{4}q'^2qq'x}\ ,\ \pi_2=\sqrt{q'^2+\frac{1}{4}q'^2qq'x}\ , \tag{4.54}$$

and $G_{\alpha'\alpha}(q'qx)$ is a purely geometrical quantity.

The three-nucleon propagator in partial-wave basis is

$$\langle pq\alpha|G_0|p'q'\alpha'\rangle = \frac{1}{E-\frac{p^2}{m}-\frac{3}{4m}q^2}\frac{\delta(q-q')}{qq'}\frac{\delta(p-p')}{pp'}\delta_{\alpha\alpha'}\ . \tag{4.55}$$

Inserting decompositions (4.50) and (4.51) and reducing momenta integrations with help of δ-functions one gets

$$\begin{aligned}\langle pq\alpha|T|\phi\rangle =& \sum_{\alpha'}\int\limits_{-1}^{1}dx\frac{\tilde{t}_{\tilde{\alpha}\tilde{\alpha}'}(p,\pi_1,E-(3/4)q^2)}{\pi_1^{l'}}\sum_{\alpha''}\delta_{\alpha''\alpha_d}G_{\alpha'\alpha''}(q,q_0,x)\frac{\varphi_{l''}(\pi_2)}{\pi_2^{l''}}C_{\alpha''}^{m_dm_N} \\ &+\sum_{\alpha'}\sum_{\alpha''}\int\limits_0^\infty dq'q'^2\int\limits_{-1}^{1}dx\frac{\tilde{t}_{\tilde{\alpha}\tilde{\alpha}'}(p,\pi_1,E-(3/4)q^2)}{\pi_1^{l'}} \\ &\times G_{\alpha'\alpha''}(qq'x)\frac{1}{E+i\varepsilon-q^2/m-q'^2/m-qq'x/m}\frac{\langle\pi_2q'\alpha''|T|\phi\rangle}{\pi_2^{l''}}\ ,\end{aligned} \tag{4.56}$$

where

$$C_{\alpha''}^{m_d m_N} = \sqrt{\frac{2\lambda+1}{4\pi}} C\left(\lambda \frac{1}{2} I, 0 m_N\right) C\left(1IJ, m_d m_N\right) \ , \tag{4.57}$$

and α_d denotes the set of discrete quantum numbers for the 2N subsystem containing the deuteron quantum numbers $l = 0, 2$, $s = 1$, $j = 1$, and $t = 0$.

In all my numerical 3N calculations, Eq. (4.46) is solved numerically by generating its Neumann series which is next summed up using the Padè method [2, 98]. The partial wave basis comprising 3N states includes all states with the two-body subsystem total angular momentum $j \leq 5$ and the total 3N angular momentum $J \leq \frac{25}{2}$. This guarantes convergence of predictions with respect to the total angular momenta. The total number of three-nucleon channels states $|\alpha\rangle$ for gieven J amounts up to 142. The range and size of grid points representing momenta p and q are chosen adjusted separately for each of the potential models. I use grids of 32 p points in the range 0-40 fm^{-1} and 37 q points in the range 0-25 fm^{-1} in case of for the chiral SMS force and the OPE-Gaussian potential.

4.3.1 3N scattering observables

The 3N scattering processes are characterized by a large set of spin-observables. In addition to the polarized differential cross section and the vector analyzing powers of nucleons, there are also vector and tensor analyzing powers of the deuteron. Further information on the dynamics can be found from the spin transfer and the spin-correlation coefficients. In total, there are 55 different observables for the elastic scattering. By solving Eqs. (4.56) and (4.43) one find the elastic transition amplitude U. It is directly related to the physical elastic scattering amplitude taking into account various polarization states

$$M_{ij} \equiv -\frac{2}{3} m (2\pi)^2 \langle \phi' | U | \phi \rangle = -\frac{2}{3} m (2\pi)^2 \left\langle \phi'_j | U | \phi_i \right\rangle \ , \tag{4.58}$$

where i, j denote denote the initial and final spin states, respectively. From M_{ij} any elastic 3N observable can be computed.

For example, the polarized differential cross section for the elastic Nd scattering in the c.m.s. equals

$$\frac{d\sigma}{d\Omega} = |M_{m'_d m'_N m_d m_N}(\vec{q}', \vec{q}_0)|^2 \ , \tag{4.59}$$

where $\vec{q}_0$ is the relative momentum of the incident nucleon with respect to the deuteron, and $\vec{q}'$ describes the same momentum in the final state. More general representation for the spin-averaged (unpolarized) differential cross section is given by

$$\frac{d\sigma}{d\Omega} \equiv I_0 = \frac{1}{6} \mathrm{Tr}(M M^\dagger) \ , \tag{4.60}$$

with trace taken over spin states.

In case of the deuteron breakup, the five-fold differential cross section in the c.m.s. is given as

$$\frac{d^5\sigma}{d\hat{p} d\hat{q} dq} = \frac{(2\pi)^4 m^2}{3 q_0} p q^2 | \langle \phi_0 | U_0 | \phi \rangle |^2 \ . \tag{4.61}$$

In practice, depending on the kinematically allowed configuration, $\frac{d^5\sigma}{d\hat{p} d\hat{q} dq}$ can be expressed as a function of laboratory scattering angles, $\frac{d^5\sigma}{d\Omega_1 d\Omega_2 dE}$, and the arc-length of the S-

curve, $\frac{d^5\sigma}{d\Omega_1 d\Omega_2 dS}$, see Ref. [2]. In principle, this is also valid for to polarized various 3N breakup polarization observables.

The same representation allows to define the spin observables [2]. The initial state polarization of the nucleon leads to the definition of the nucleon analyzing powers

$$A_k(N) \equiv \frac{\mathrm{Tr}(M\sigma_k M^\dagger)}{\mathrm{Tr}(MM^\dagger)} \ . \tag{4.62}$$

Using the common convention to choose the scattering plane as the $x-z$ plane and the y axis pointing to the direction $\vec{k}_{in} \times \vec{k}_{out}$, where $\vec{k}_{in}$ and $\vec{k}_{out}$ are the momenta of the incoming and outgoing nucleons, respectively, results in non-zero the nucleon vector analyzing power $A_y(N)$, while $A_x(N) = A_z(N) = 0$.

The deuteron vector and the tensor polarizations of the deuteron in the initial state leads to the vector A_i and the tensor A_{jk} analyzing powers of the deuteron, respectively,

$$A_i = \frac{\mathrm{Tr}(M\mathcal{P}_i M^\dagger)}{MM^\dagger} \ , \ A_{jk} = \frac{\mathrm{Tr}(M\mathcal{P}_{jk} M^\dagger)}{MM^\dagger} \ , \tag{4.63}$$

where $\mathcal{P}_i$ is the polarization vector and $\mathcal{P}_{jk}$ is the polarization tensor. The parity conservation reduces the number of observables resulting in only vector and three tensor analyzing powers

$$iT_{11} = \frac{\sqrt{3}}{2} A_y \ , \ T_{20} = \frac{1}{\sqrt{2}} A_{zz} \ , \ T_{21} = -\frac{1}{\sqrt{3}} A_{xz} \ , \ T_{22} = \frac{1}{2\sqrt{3}} (A_{xx} - A_{yy}) \ . \tag{4.64}$$

When, both the incident nucleon and the deuteron are polarized in the initial state various spin-correlation coefficients $C_{j,k}$ and $C_{jk,i}$ occures. In the case when one particle s polarized in the initial state and one in the final state we deal with the spin transfer coefficients $K_k^{l'}$ and $K_k^{li'}$.

All those above-mentioned quantities depend on the scattering angle and reaction energy. Extending the above definitions one can define the spin observables in the deuteron breakup process for which the number of 3N observables is much greater than for the elastic scattering.

Bibliography

[1] H. Witała, W. Glöckle, J. Golak, A. Nogga, H. Kamada, R. Skibiński, and J. Kuroś-Żołnierczuk. Nd elastic scattering as a tool to probe properties of 3N forces. *Physical Review C - Nuclear Physics*, 63(2):12, 2001.

[2] W. Glöckle, H. Witała, D. Hüber, H. Kamada, and J. Golak. The three-nucleon continuum: achievements, challenges and applications. *Phys. Rept.*, 274:107–285, 1998.

[3] C.R. Howell, W. Tornow, H.R. Setze, R.T. Braun, D.E.Gonzalez Trotter, C.D. Roper, R.S. Pedroni, S.M. Grimes, C.E. Brient, N. Al-Niemi, F.C. Goeckner, and G. Mertens. Resolution of discrepancy between backward angle cross-section data for neutron-deuteron elastic scattering. *Few-Body Systems*, 16(3):127–142, 1994.

[4] St. Kistryn, E. Stephan, A. Biegun, K. Bodek, A. Deltuva, E. Epelbaum, K. Ermisch, W. Glöckle, J. Golak, N. Kalantar-Nayestanaki, H. Kamada, M. Kiš, B. Kłos, A. Kozela, J. Kuroś-Znierczuk, M. Mahjour-Shafiei, U. G. Meißner, A. Micherdzińska, A. Nogga, P. U. Sauer, R. Skibiński, R. Sworst, H. Witała, J. Zejma, and W. Zipper. Systematic study of three-nucleon force effects in the cross section of the deuteron-proton breakup at 130 MeV. *Physical Review C - Nuclear Physics*, 72(4):1–25, 2005.

[5] B. V. Przewoski, H. O. Meyer, J. T. Balewski, W. W. Daehnick, J. Doskow, W. Haeberli, R. Ibald, B. Lorentz, R. E. Pollock, P. V. Pancella, F. Rathmann, T. Rinckel, Swapan K. Saha, B. Schwartz, P. Thörngren-Engblom, A. Wellinghausen, T. J. Whitaker, and T. Wise. Analyzing powers and spin correlation coefficients for $p + d$ elastic scattering at 135 and 200 MeV. *Physical Review C - Nuclear Physics*, 74(6):1–21, 2006.

[6] G.J. Weisel, W. Tornow, A.S. Crowell, J.H. Esterline, G.M. Hale, C.R. Howell, P.D. O'Malley, J.R. Tompkins, and H. Witała. Neutron-deuteron analyzing power data at $E_n = 22.5$ MeV. *Physical Review C - Nuclear Physics*, 89(5):1–7, 2014.

[7] K. Sekiguchi, H. Witała, T. Akieda, D. Eto, H. Kon, Y. Wada, A. Watanabe, S. Chebotaryov, M. Dozono, J. Golak, H. Kamada, S. Kawakami, Y. Kubota, Y. Maeda, K. Miki, E. Milman, A. Ohkura, H. Sakai, S. Sakaguchi, N. Sakamoto, M. Sasano, Y. Shindo, R. Skibiński, H. Suzuki, M. Tabata, T. Uesaka, T. Wakasa, K. Yako, T. Yamamoto, Y. Yanagisawa, and J. Yasuda. Complete set of deuteron analyzing powers from d - p elastic scattering at 190 MeV/nucleon. *Physical Review C*, 96(6):1–8, 2017.

[8] Editorial: Uncertainty estimates. *Physical Review A - Atomic, Molecular, and Optical Physics*, 83(4):40001, 2011.

[9] P. Reinert, H. Krebs, and E. Epelbaum. Semilocal momentum-space regularized chiral two-nucleon potentials up to fifth order. *European Physical Journal A*, 54(5):1–49, 2018.

[10] R. Navarro Pérez, J.E. Amaro, and E. Ruiz Arriola. Statistical error analysis for phenomenological nucleon-nucleon potentials. *Physical Review C - Nuclear Physics*, 89(6):1–20, 2014.

[11] R. Skibiński, Yu. Volkotrub, J. Golak, K. Topolnicki, and H. Witała. Theoretical uncertainties of the elastic nucleon-deuteron scattering observables. *Physical Review C*, 98(1):1–15, 2018.

[12] Yuriy Volkotrub, Jacek Golak, Roman Skibinski, Kacper Topolnicki, Henryk Witala, Evgeny Epelbaum, Hermann Krebs, and Patrick Reinert. Uncertainty of three-nucleon continuum observables arising from uncertainties of two-nucleon potential parameters. *Journal of Physics G: Nuclear and Particle Physics*, 2020.

[13] S. Binder, A. Calci, E. Epelbaum, R.J. Furnstahl, J. Golak, K. Hebeler, H. Kamada, H. Krebs, J. Langhammer, S. Liebig, et al. Few-nucleon systems with state-of-the-art chiral nucleon-nucleon forces. *Physical Review C*, 93(4):044002, 2016.

[14] S. Binder, A. Calci, E. Epelbaum, R.J. Furnstahl, J. Golak, K. Hebeler, T. Hüther, H. Kamada, H. Krebs, P. Maris, et al. Few-nucleon and many-nucleon systems with semilocal coordinate-space regularized chiral nucleon-nucleon forces. *Physical Review C*, 98(1):014002, 2018.

[15] J.A. Melendez, S. Wesolowski, and R.J. Furnstahl. Bayesian truncation errors in chiral effective field theory: nucleon-nucleon observables. *Physical Review C*, 96(2):024003, 2017.

[16] S.R. Beane, W. Detmold, K. Orginos, and M.J. Savage. Nuclear physics from lattice QCD. *Progress in Particle and Nuclear Physics*, 66(1):1–40, 2011.

[17] S. Aoki. Hadron interactions in lattice QCD. *Progress in Particle and Nuclear Physics*, 66(4):687–726, 2011.

[18] S.R. Beane, E. Chang, S.D. Cohen, W. Detmold, H.W. Lin, T.C. Luu, K. Orginos, A. Parreño, M.J. Savage, and A. Walker-Loud. Light nuclei and hypernuclei from quantum chromodynamics in the limit of SU(3) flavor symmetry. *Physical Review D - Particles, Fields, Gravitation and Cosmology*, 87(3):1–20, 2013.

[19] K. Orginos, A. Parreno, M.J. Savage, S.R. Beane, E. Chang, W. Detmold, NPLQCD Collaboration, et al. Two nucleon systems at $m_\pi \sim 450$ MeV from lattice QCD. *Physical Review D*, 92(11):114512, 2015.

[20] Ning Li, S. Elhatisari, E. Epelbaum, Dean Lee, Bing-Nan Lu, and Ulf-G Meißner. Neutron-proton scattering with lattice chiral effective field theory at next-to-next-to-next-to-leading order. *Physical Review C*, 98(4):044002, 2018.

[21] W. Leidemann and G. Orlandini. Modern *ab initio* approaches and applications in few-nucleon physics with A $\geq$ 4. *Progress in Particle and Nuclear Physics*, 68:158–214, 2013.

[22] A. Nogga, H. Kamada, and W. Gloeckle. Modern nuclear force predictions for the α particle. *Physical Review Letters*, 85(5):944, 2000.

[23] J. Carlson, S. Gandolfi, F. Pederiva, Steven C. Pieper, R. Schiavilla, K.E. Schmidt, and Robert B. Wiringa. Quantum monte carlo methods for nuclear physics. *Reviews of Modern Physics*, 87(3):1067, 2015.

[24] P. Navrátil, S. Quaglioni, G. Hupin, C. Romero-Redondo, and A. Calci. Unified *ab initio* approaches to nuclear structure and reactions. *Physica Scripta*, 91(5):053002, 2016.

[25] P. Maris, M.A. Caprio, and J.P. Vary. Emergence of rotational bands in *ab initio* no-core configuration interaction calculations of the Be isotopes. *Physical Review C*, 91(1):014310, 2015.

[26] T. Fukui, L. De Angelis, Y.Z. Ma, L. Coraggio, A. Gargano, N. Itaco, and F.R. Xu. Realistic shell-model calculations for p-shell nuclei including contributions of a chiral three-body force. *Physical Review C*, 98(4):044305, 2018.

[27] E. Epelbaum, J. Golak, K. Hebeler, T. Hüther, H. Kamada, H. Krebs, P. Maris, Ulf-G Meißner, A. Nogga, R. Roth, et al. Few-and many-nucleon systems with semilocal coordinate-space regularized chiral two-and three-body forces. *Physical Review C*, 99(2):024313, 2019.

[28] S.K. Bogner, R.J. Furnstahl, and A. Schwenk. From low-momentum interactions to nuclear structure. *Progress in Particle and Nuclear Physics*, 65(1):94–147, 2010.

[29] H. Hergert, S.K. Bogner, T.D. Morris, A. Schwenk, and K. Tsukiyama. The in-medium similarity renormalization group: A novel *ab initio* method for nuclei. *Physics Reports*, 621:165–222, 2016.

[30] A. Kievsky, S. Rosati, M. Viviani, L.E Marcucci, and L. Girlanda. A high-precision variational approach to three-and four-nucleon bound and zero-energy scattering states. *Journal of Physics G: Nuclear and Particle Physics*, 35(6):063101, 2008.

[31] L.E. Marcucci, A. Kievsky, L. Girlanda, S. Rosati, and M. Viviani. N-d elastic scattering using the hyperspherical harmonics approach with realistic local and nonlocal interactions. *Physical Review C*, 80(3):034003, 2009.

[32] L.E. Marcucci, J. Dohet-Eraly, L. Girlanda, A. Gnech, A. Kievsky, and M. Viviani. The hyperspherical harmonics method: a tool for testing and improving nuclear interaction models. *arXiv preprint arXiv:1912.09751*, 2019.

[33] L.D. Faddeev. Scattering theory for a three-particle system. In *Fifty Years of Mathematical Physics: Selected Works of Ludwig Faddeev*, pages 37–42. World Scientific, 2016.

[34] O.A. Rubtsova, V.N. Pomerantsev, V.I. Kukulin, and A. Faessler. Three-body breakup within the fully discretized Faddeev equations. *Physical Review C*, 86(3):034004, 2012.

[35] A.C. Fonseca and A. Deltuva. Numerical exact *ab initio* four-nucleon scattering calculations: from dream to reality. *Few-Body Systems*, 58(2):46, 2017.

[36] A. Deltuva, A.C. Fonseca, and P.U. Sauer. Coulomb force effects in few-nucleon systems. *Few-Body Systems*, 60(2):29, 2019.

[37] Rimantas Lazauskas. Solution of the n-He^4 elastic scattering problem using the Faddeev-Yakubovsky equations. *Physical Review C*, 97(4):044002, 2018.

[38] C.W. Johnson, K.D. Launey, N. Auerbach, S. Bacca, B.R. Barrett, C. Brune, M.A. Caprio, P. Descouvemont, W.H. Dickhoff, Ch. Elster, et al. From bound states to the continuum. *arXiv preprint arXiv:1912.00451*, 2019.

[39] G. Raciti, G. Cardella, M. De Napoli, E. Rapisarda, F. Amorini, and C. Sfienti. Experimental evidence of He2 decay from Ne18 excited states. *Physical Review Letters*, 100(19):2–5, 2008.

[40] Hideki Yukawa. On the interaction of elementary particles. i. *Proceedings of the Physico-Mathematical Society of Japan. 3rd Series*, 17:48–57, 1935.

[41] W.N. Cottingham, M. Lacombe, B. Loiseau, J.M. Richard, and R. Vinh Mau. Nucleon-nucleon interaction from pion-nucleon phase-shift analysis. *Physical Review D*, 8(3):800, 1973.

[42] R. Machleidt, K. Holinde, and Ch. Elster. The Bonn meson-exchange model for the nucleon—nucleon interaction. *Physics Reports*, 149(1):1–89, 1987.

[43] V.G.J. Stoks, R.A.M. Klomp, M.C.M. Rentmeester, and J.J. De Swart. Partial-wave analysis of all nucleon-nucleon scattering data below 350 MeV. *Physical Review C*, 48(2):792, 1993.

[44] Ruprecht Machleidt. Nuclear forces. *Scholarpedia*, 9(1), 2014.

[45] Mohammad Naghdi. Nucleon-nucleon interaction: A typical/concise review. *Physics of Particles and Nuclei*, 45(5):924–971, 2014.

[46] V.I. Zhaba. Deuteron: properties and analytical forms of wave function in coordinate space. *arXiv preprint arXiv:1706.08306*, 2017.

[47] Ruprecht Machleidt. Historical perspective and future prospects for nuclear interactions. *International Journal of Modern Physics E*, 26(11):1730005, 2017.

[48] Vittorio Somà. From the liquid drop model to lattice QCD: A brief history of nuclear interactions. *European Physical Journal Plus*, 133(10):1–22, 2018.

[49] R.B. Wiringa, V.G.J. Stoks, and R. Schiavilla. Accurate nucleon-nucleon potential with charge-independence breaking. *Physical Review C*, 51(1):38–51, 1995.

[50] R. Machleidt. High-precision, charge-dependent Bonn nucleon-nucleon potential. *Physical Review C - Nuclear Physics*, 63(2):32, 2001.

[51] R. Navarro Pérez, J.E. Amaro, and E. Ruiz Arriola. Coarse-grained potential analysis of neutron-proton and proton-proton scattering below the pion production threshold. *Physical Review C - Nuclear Physics*, 88(6):1–31, 2013.

[52] Steven Weinberg. Nuclear forces from chiral lagrangians. *Physics Letters B*, 251(2):288–292, 1990.

[53] Steven Weinberg. Effective chiral lagrangians for nucleon-pion interactions and nuclear forces. *Nuclear Physics B*, 363(1):3–18, 1991.

[54] E. Epelbaum, H. Krebs, and P. Reinert. High-Precision Nuclear Forces From Chiral EFT: State-of-the-Art, Challenges, and Outlook. *Frontiers in Physics*, 8(April):1–30, 2020.

[55] E. Epelbaum, H. Krebs, and U. G. Meißner. Improved chiral nucleon-nucleon potential up to next-to-next-to-next-to-leading order. *European Physical Journal A*, 51(5), 2015.

[56] D. R. Entem, R. Machleidt, and Y. Nosyk. High-quality two-nucleon potentials up to fifth order of the chiral expansion. *Physical Review C*, 96(2):1–19, 2017.

[57] R.J. Furnstahl, N. Klco, D.R. Phillips, and S. Wesolowski. Quantifying truncation errors in effective field theory. *Physical Review C - Nuclear Physics*, 92(2), 2015.

[58] E. Epelbaum, J. Golak, K. Hebeler, H. Kamada, H. Krebs, U-G. Meißner, A. Nogga, P. Reinert, R. Skibiński, K. Topolnicki, et al. Towards high-order calculations of three-nucleon scattering in chiral effective field theory. *The European Physical Journal A*, 56(3):1–14, 2020.

[59] Evgeny Epelbaum. Nuclear forces from chiral effective field theory: a primer. *arXiv preprint arXiv:1001.3229*, 2010.

[60] Evgeny Epelbaum. Few-nucleon forces and systems in chiral effective field theory. *Progress in Particle and Nuclear Physics*, 57(2):654–741, 2006.

[61] E. Epelbaum, H.W. Hammer, and Ulf.G. Meißner. Modern theory of nuclear forces. *Reviews of Modern Physics*, 81(4):1773–1825, 2009.

[62] E. Epelbaum, H. Krebs, and U. G. Meißner. Precision Nucleon-Nucleon Potential at Fifth Order in the Chiral Expansion. *Physical Review Letters*, 115(12):1–5, 2015.

[63] R. Machleidt and D. R. Entem. Chiral effective field theory and nuclear forces. *Physics Reports*, 503(1):1–75, 2011.

[64] R. Machleidt. Nuclear Forces from Chiral Effective Field Theory: Achievements and Challenges. *Few-Body Systems*, 54(1-4):5–10, 2013.

[65] R. Machleidt and F. Sammarruca. Chiral EFT based nuclear forces: Achievements and challenges. *Physica Scripta*, 91(8), 2016.

[66] R. Machleidt. Consistent, high-quality two-nucleon potentials up to fifth order of the chiral expansion. *Journal of Physics: Conference Series*, 966(1), 2018.

[67] J.R. Bergervoet, P.C. Van Campen, W.A. Van Der Sanden, and J.J. De Swart. Phase shift analysis of 0-30 MeV pp scattering data. *Physical Review C*, 38(1):15–50, 1988.

[68] A. Nogga, D. Hüber, H. Kamada, and W. Glöckle. Triton binding energies for modern nn forces and the π-π exchange three-nucleon force. *Physics Letters B*, 409(1-4):19–25, 1997.

[69] A. Nogga, A. Kievsky, H. Kamada, W. Glöckle, L.E. Marcucci, S. Rosati, and M. Viviani. Three-nucleon bound states using realistic potential models. *Physical Review C*, 67(3):034004, 2003.

[70] R. Navarro Pérez, E. Garrido, J.E. Amaro, and E. Ruiz Arriola. Triton binding energy with realistic statistical uncertainties. *Physical Review C*, 90(4):047001, 2014.

[71] D.R. Entem, R. Machleidt, and H. Witała. Chiral NN model and A_y-puzzle. *Physical Review C*, 65(6):064005, 2002.

[72] H. Witała and W. Glöckle. On the discrepancies in the low-energy neutron–deuteron breakup. *Journal of Physics G: Nuclear and Particle Physics*, 37(6):064003, 2010.

[73] H. Witała and W. Glöckle. The *nn* quasifree *nd* breakup cross section: Discrepancies with theory and implications for the $^1S_0$ nn force. *Physical Review C*, 83(3):034004, 2011.

[74] S.A. Coon, M.D. Scadron, P.C. McNamee, Bruce R. Barrett, D.W.E. Blatt, and B.H.J. McKellar. The two-pion-exchange three-nucleon potential and nuclear matter. *Nuclear Physics A*, 317(1):242–278, 1979.

[75] S.A. Coon and W. Glöckle. Two-pion-exchange three-nucleon potential: Partial wave analysis in momentum space. *Physical Review C*, 23(4):1790, 1981.

[76] S.A. Coon and H.K. Han. Reworking the tucson-melbourne three-nucleon potential. *Few-Body Systems*, 30(1-2):131–141, 2001.

[77] B.S. Pudliner, V.R. Pandharipande, J. Carlson, S.C. Pieper, and Robert B. Wiringa. Quantum monte carlo calculations of nuclei with A$<\tilde{}$ 7. *Physical Review C*, 56(4):1720, 1997.

[78] E. Epelbaum, H. Kamada, A. Nogga, H. Witała, W. Gloeckle, and Ulf-G. Meissner. Three-and four-nucleon systems from chiral effective field theory. *Physical review letters*, 86(21):4787, 2001.

[79] R. Skibiński, J. Golak, K. Topolnicki, H. Witała, E. Epelbaum, W. Glöckle, H. Krebs, A. Nogga, and H. Kamada. Triton with long-range chiral N3LO three-nucleon forces. *Physical Review C*, 84(5):054005, 2011.

[80] L. Girlanda, A. Kievsky, and M. Viviani. Subleading contributions to the three-nucleon contact interaction. *Physical Review C*, 84(1):014001, 2011.

[81] A.C. Phillips. Consistency of the low-energy three-nucleon observables and the separable interaction model. *Nuclear Physics A*, 107(1):209–216, 1968.

[82] K. Sekiguchi, H. Sakai, H. Witała, W. Glöckle, J. Golak, M. Hatano, H. Kamada, H. Kato, Y. Maeda, J. Nishikawa, et al. Complete set of precise deuteron analyzing powers at intermediate energies: comparison with modern nuclear force predictions. *Physical Review C*, 65(3):034003, 2002.

[83] A. Ekström, G. Baardsen, C. Forssén, G. Hagen, M. Hjorth-Jensen, G.R. Jansen, R. Machleidt, W. Nazarewicz, T. Papenbrock, J. Sarich, et al. Optimized chiral nucleon-nucleon interaction at next-to-next-to-leading order. *Physical review letters*, 110(19):192502, 2013.

[84] R. Navarro Pérez, J.E. Amaro, and E. Ruiz Arriola. Low-energy chiral two-pion exchange potential with statistical uncertainties. *Physical Review C*, 91(5):054002, 2015.

[85] V.G.J. Stoks, R.A.M. Klomp, M.C.M. Rentmeester, and J.J. De Swart. Partial-wave analysis of all nucleon-nucleon scattering data below 350 MeV. *Physical Review C*, 48(2):792–815, 1993.

[86] E. Arriola Ruiz and R. Navarro Pérez. *Private communication*, 2017.

[87] R. Navarro Pérez, J. E. Amaro, and E. Ruiz Arriola. Erratum: Coarse-grained potential analysis of neutron-proton and proton-proton scattering below the pion production threshold (Physical Review C - Nuclear Physics (2013) 88 (064002)). *Physical Review C - Nuclear Physics*, 91(2):24–26, 2015.

[88] Franz Gross and Alfred Stadler. Covariant spectator theory of np scattering: Phase shifts obtained from precision fits to data below 350 MeV. *Physical Review C*, 78(1):014005, 2008.

[89] R. Navarro Pérez, E. Garrido, J.E. Amaro, and E. Ruiz Arriola. Triton binding energy with realistic statistical uncertainties. *Physical Review C - Nuclear Physics*, 90(4):1–5, 2014.

[90] M. Hoferichter, Jacobo R. de Elvira, B. Kubis, and Ulf-G Meißner. Matching pion-nucleon roy-steiner equations to chiral perturbation theory. *Physical review letters*, 115(19):192301, 2015.

[91] Wolfram Research, Inc. Mathematica, Version 11.3. Champaign, IL, 2018.

[92] R. Navarro Pérez, A. Nogga, J. E. Amaro, and E. Ruiz Arriola. Binding in light nuclei: Statistical NN uncertainties vs Computational accuracy. *Journal of Physics: Conference Series*, 742(1), 2016.

[93] Johannes Kirscher, Harald W Grießhammer, Deepshikha Shukla, and Hartmut M Hofmann. Universal correlations in pion-less eft with the resonating group method: Three and four nucleons. *The European Physical Journal A*, 44(2):239–256, 2010.

[94] A. Kievsky, M. Viviani, D. Logoteta, I. Bombaci, and L. Girlanda. Correlations imposed by the unitary limit between few-nucleon systems, nuclear matter, and neutron stars. *Physical review letters*, 121(7):072701, 2018.

[95] J.A. Tjon. Bound states of 4he with local interactions. *Physics Letters B*, 56(3):217 – 220, 1975.

[96] A. R. Edmonds. The angular momentum in quantum mechanics. *Princeton University Press*, 1960.

[97] C. Van Der Leun and C. Alderliesten. The deuteron binding energy. *Nuclear Physics A*, 380(2):261–269, 1982.

[98] Walter Glöckle. *The quantum mechanical few-body problem*. Springer-Verlag Berlin Heidelberg, 1983.

[99] Charlotte Elster. Lectures on few body systems. Available online at http://www.phy.ohio.edu/ elster/phys755/index.html.

[100] H.P. Stapp, T.J. Ypsilantis, and N. Metropolis. Phase-shift analysis of 310 Mev proton-proton scattering experiments. *Phys. Rev.*, 105:302–310, Jan 1957.

[101] H Witała, W Glöckle, and Th. Cornelius. Nucleon-induced deuteron breakup: analysis of 14.1 MeV data by rigorous Faddeev calculations with meson-exchange NN interactions. *Physical Review C*, 39(2):384, 1989.

[102] H. Witała, J. Golak, R. Skibiński, K. Topolnicki, E. Epelbaum, K. Hebeler, H. Kamada, H. Krebs, U.-G. Meißner, and A. Nogga. Role of the total isospin 3/2 component in three-nucleon reactions. *Few-Body Systems*, 57(12):1213–1225, 2016.